ARL 62-374

RESEARCH IN THE MEASUREMENTS AND THEORY OF PLASMOIDS AND THEIR APPLICATIONS TO MISSILES AND SATELLITE TECHNOLOGY

LAWRENCE C. SCHOLZ

ILLINOIS INSTITUTE OF TECHNOLOGY
CHICAGO, ILLINOIS

JULY 1962

AERONAUTICAL RESEARCH LABORATORIES
OFFICE OF AEROSPACE RESEARCH
UNITED STATES AIR FORCE

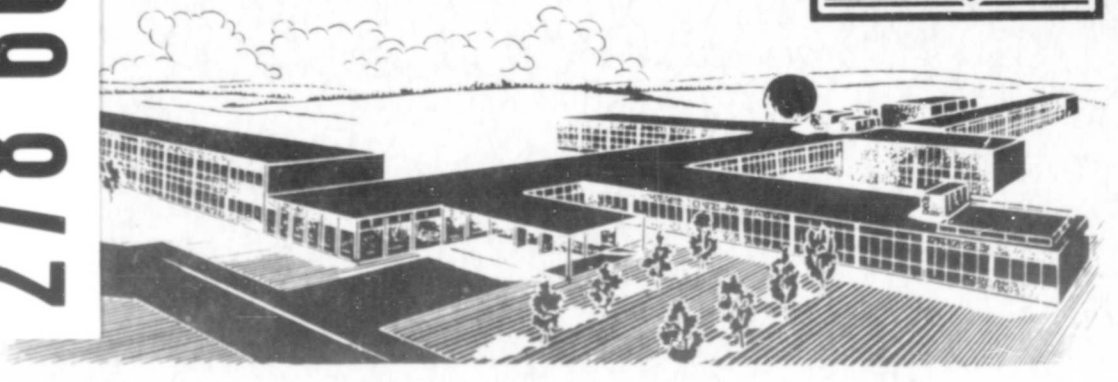

NOTICES

When Government drawings, specifications, or other data are used for any purpose other than in connection with a definitely related Government procurement operation, the United States Government thereby incurs no responsibility nor any obligation whatsoever; and the fact that the Government may have formulated, furnished, or in any way supplied the said drawings, specifications, or other data, is not to be regarded by implication or otherwise as in any manner licensing the holder or any other person or corporation, or conveying any rights or permission to manufacture, use, or sell any patented invention that may in any way be related thereto.

- - - - - - - - - -

Qualified requesters may obtain copies of this report from the Armed Services Technical Information Agency, (ASTIA), Arlington Hall Station, Arlington 12, Virginia.

- - - - - - - - - -

This report has been released to the Office of Technical Services, U. S. Department of Commerce, Washington 25, D. C. for sale to the general public.

Stock available at OTS $ 1.75

- - - - - - - - - -

Copies of ARL Technical Documentary Reports should not be returned to Aeronautical Research Laboratory unless return is required by security considerations, contractual obligations, or notices on a specific document.

AF-WP-L-APR 62 100

ARL 62-374

RESEARCH IN THE MEASUREMENTS AND THEORY OF PLASMOIDS AND THEIR APPLICATIONS TO MISSILES AND SATELLITE TECHNOLOGY

LAWRENCE C. SCHOLZ

ARMOUR RESEARCH FOUNDATION
OF
ILLINOIS INSTITUTE OF TECHNOLOGY
CHICAGO, ILLINOIS

JULY 1962

Contract AF 33(616)-5791
Project 7073
Task 7073-03

AERONAUTICAL RESEARCH LABORATORIES
OFFICE OF AEROSPACE RESEARCH
UNITED STATES AIR FORCE
WRIGHT-PATTERSON AIR FORCE BASE, OHIO

400 - August 1962 - 42-1875

FOREWORD

This report was prepared by the Armour Research Foundation of Illinois Institute of Technology, and is the final report on Contract No. AF 33(616)-5791, Project 7073, Task 7073-03. The title of which is Research in the Measurements and Theory of Plasmoids and Their Applications to Missiles and Satellite Technology. The project had as its main concern the generation and investigation of spark derived plasmoids and their possible applications in an upper atmosphere environment. The program was administered by the Aeronautical Research Laboratories, Office of Aerospace Research, and was monitored by Dr. W. G. Braun. Mr. L. C. Scholz was the principle investigator in the last year of the contract.

The contract period extended from 1 June 1958 to 15 September 1961. During the course of the contract both theoretical and experimental programs were carried out. The most recent work, for the period June 1960 to September 1961, was mainly experimental and constitutes the major part of this report, although a summary of the past work is also given.

Mr. J. T. Jones built much of the electronic equipment and assisted in the experimental program. The following people made substantial contributions during the course of the work. Theoretical - Mr. T. Englehardt, Mr. Val Pratt, and Dr. M. S. Sodha. Experimental - Mr. D. DeGeeter and Mr. R. L. Watkins. The theoretical work has not been included in this report, but may be found in earlier reports under this contract number.

ABSTRACT

High-speed metal spark-derived plasmoids have been produced in a magnetic field under high vacuum conditions (10^{-6} torr). The velocity and other properties of these plasmoids have been measured under a variety of conditions. Interaction of the plasmoids with obstacles, the magnetic field and other plasmoids has also been investigated. The work presented in this report is mainly experimental, although a theoretical program was also carried out.

Electrode processes were investigated and a concept of a "best" material is discussed. However, this is a tentative conclusion and further work is needed.

Special equipment developed during the program is discussed. This includes capacitor discharge circuits and a high speed camera with an image convertor tube as an electronic shutter.

TABLE OF CONTENTS

LIST OF ILLUSTRATIONS

LIST OF ILLUSTRATIONS (Continued)

LIST OF ILLUSTRATIONS (Continued)

CONCLUSIONS AND GENERAL COMMENTS

These general comments and conclusions are primarily the result of our own experiments and work, but also take into consideration other experiments reported in the literature, a representative list of which may be seen in Section I of the bibliography at the end of the paper.

Briefly we may say that the plasma entities or plasmoids produced by the button-spark source are amorphous jets of plasma moving with a velocity of the order of 5×10^6 cm/sec across a magnetic field of some 4,000 oersteds. The velocity and character of the plasmoid are highly dependent on the magnetic field and discharge current. With zero background field there is no plasmoid formation, but the ionized plasma material has an apparent velocity about an order of magnitude higher then the plasmoid. The internal properties of the plasmoid are little known and no good quantitative theory exists. Although the velocity was fairly constant during our measurements there is reason to expect that the internal characteristics are not uniform from discharge to discharge.

Button-formed plasmoids themselves do not seem to have lived up to their initial promise, and while the Bostick plasmoid system is still interesting because of its high velocities and constructional simplicity, there do exist many better systems for quantitative experiments. As it has been shown the earlier concepts of the plasmoid, such as structure and stability have been discounted or greatly modified and present interest is in other properties such as its conductivity and interaction with the magnetic field. Therefore we would recommend that future work concentrate on the acceleration and motion of the plasmoid in a magnetic field and use more reproducible and analytically tractable systems that provide better geometric constraints on the plasmoid entity.

SUMMARY OF PREVIOUS WORK

The initial concepts of this project were very broad. They were conceived when plasmoids were little understood and the term was highly specialized. The term plasmoid has altered its meaning during the course of this work. The original concept was of a highly structured, quasi-stable finite plasma. This was the plasmoid of Bosticks early work.[1, 2, 3] More recent observations by ourselves and others[4, 5, 6] have led us away from this earlier concept. We still retain the term plasmoid as a generic term for any finite plasma existing as a somewhat independent entity. This separates it, say from a plasma filling a region in a discharge tube. The term no longer holds any implication as to its method of production or internal characteristics.

The early phase of this program had as its broad objective the theoretical and experimental studies of plasmoids, including their generation,

Manuscript released by the author 16 April 1962 for publication as an ARL Technical Documentary Report.

properties and uses. This proved to be rather ambitious. A strong theoretical program designed to find stable magnetized-plasma configurations ran into some formidable mathematical obstacles, with indications that it would not be successful except for certain very special cases of little general interest. The experimental work was directed towards construction of a suitable apparatus with the required diagnostic equipment. This is reported in ARF 1121-4, the first annual report.

The second phase of the work was partially theoretical, and mainly experimental. The theoretical approach was of a more general nature and resulted in a publication by Dr. M. S. Sodha* on the transport properties of a slightly ionized gas. There was also a further attempt at the stability problem from a numerical basis using computer techniques. This to proved too formidable, and was discarded when it was found that no assurance of convergence could be given. The experimental program included the construction of a high speed image converter camera and an attempt to study the plasma properties using microwave absorption techniques. The microwave experiment was frustrated by three factors: limited equipment and frequency range, low electron density in the plasmoid requiring on the one hand a low resonant frequency, and a small plasmoid size plus high velocity requiring on the other hand a high frequency. A more sophisticated experiment using focused beams, variable frequency ranges and possibly interferometer techniques might give useful results. This work is reported in ARF 1121-8, the second annual report.

SUMMARY OF RECENT WORK DONE

In this past year the work was almost entirely experimental and a considerable improvement in the design and reliability of the equipment was made. Specific improvements include an all electronic ignitron switching in the plasmoid generator, which permits greater flexibility over a wide working range (5 - 20 kilovolts). It also provides accurate timing with very low jitter which is the key to convenient high speed photography. A satisfactory current measuring resistor was devised and installed permitting accurate determination of the magnitude and shape of the arc current. The high speed camera circuits were improved to provide faster rise time pulses (10 nanoseconds) with shorter possible exposure time (50 nanoseconds). These changes also facilitated the focusing and other adjustments of the camera.

We also made a considerable number of measurements. A series of still pictures were made with 0.2 microsecond exposure time to give an instantaneous picture of the shape and position of the plasmoid. The resolution was not as good as desired and a rough measurement was made indicating that our camera did not come up to the manufacturers specifications for the tube. The image tube failed near the end of the contract period,

---

*M. S. Sodha, "Electrical and Thermal Currents in a Slightly Ionized Gas," Phys. Rev., 119, 882 (1960).

but has since been replaced. (Unfortunately this introduced a few months wait and delayed the completion of the program). We have also taken a large number of time-integrated exposures showing the path of the plasma material through the field and around obstacles, and also its interaction with probes. The net results of the photographs and other subsidiary measurements indicate the plasmoid to be an amorphous blob of material confined in one direction by the field and whose kinetic energy content is initially greater than internal heat energy.

Using probe techniques we have measured the velocity as a function of field strength and capacitor voltage. The effect of the ambient pressure was also investigated and was found to have little effect until the pressure was above a micron.

Two other interesting topics were explored: The interaction of two plasmoids launched simultaneously on initially parallel paths and the problem of the generation and acceleration of the plasmoid. The first subject appeared to have great promise and initial experiments appeared to show a definite interaction. However, later work which was more complete and accurate did not substantiate this, so that the present conclusion is that an interaction does not occur. The generation of the plasmoid and the erosion of material from the electrodes was considered as a cold cathode arc problem and a rough study was made along these lines. Microphotographs indicate a complex arc structure at the electrodes which does not permit a simple formulation of the heat flow and other parameters; however, a very generalized idea of a "best material" was worked out.

At present the equipment is in operating order although some modification would be desirable in the image camera's high voltage supply. The addition of a streaking attachment would also be useful. The capacitor discharge circuits are working very well and are capable of switching at much higher power levels then occur with our small capacitor. The overall usefulness of the apparatus is somewhat limited, but the individual elements could be utilized for a variety of experiments.

FORMATION AND ACCELERATION OF PLASMOIDS

An analysis of the plasma production and acceleration mechanism involved in these experiments is difficult. The difficulty is not lessened by the generating system, which was patterned after that of Bostick. The "Bostick button source" consists of two parallel wires embedded in a cylinder of insulating material (see Figure 1). The actual form is not important and affects only the mechanical design of the system. The essential feature is the transient arc discharge which forms across the end of the cylinder with the two wires as electrodes. The plasma is produced by the effects of the arc current and is composed of ions evaporated from the electrodes. The acceleration is produced by the ponderomotive forces between the arc current and its own magnetic field which produces a resultant expansion of the current loop. Other electrode arrangements are much easier to analyze primarily because of their more constant arc geometry. In the Bostick method of production and acceleration of plasma,

the mass, speed, and direction of force are all variables. Other systems such as the rail or cyclindrical tube accelerators have geometrical constraints, and may indeed introduce additional constraints such as on the mass of the plasma. However, certain simple analyses concerning the system we used can be made and which we will consider below.

The experimental difficulties in a study of this sort are very great, and a reasonable opportunity should be taken to overcome them. The button type of accelerator is a poorly controlled type of device and should be discarded for an analytically simpler device, such as a tube with injected gas of known mass. Systematic measurements of various plasma accelerators indicate that the button is one of the poorest (see Plyutto[5]). Further studies with the button source would require a larger magnetic field volume to permit observations over a longer time.

THE ARC DISCHARGE

The transient arc discharge as obtained in our experiments is produced by a capacitor discharge. The equivalent circuit is shown in Figure 2 and contains the elements of both the arc and the external circuit. The arc is essentially a nonlinear circuit element with the resistance being a function of the current, and if the arc geometry is not constant (i. e. if the arc channel grows in length) then the inductance and resistance will also be a function of time. Emperical evidence in our case has shown that the nonlinearity of the arc is not important because the discharge current is controlled by the other circuit elements. Therefore, the current may be found by ordinary methods, and since the current is a simple known function of time the arc resistance and inductance may be expressed as explicit functions of time. This variation of the arc resistance and inductance are of second order when calculating the discharge current, but are extremely important in the acceleration mechanism where the $\dot{L}$ terms involve real power (see Kash[7]). An additional assumption is that radiation and retarded field effects are negligible so that simple circuit analysis methods are applicable. The current is therefore given by

$$\frac{d^2I}{dt^2} + \frac{R}{L}\frac{dI}{dt} + \frac{I}{LC} = 0 \quad .$$

The solutions I(t) are well known, and depend on the relative values of the circuit parameters. Consider first the oscillatory case: If

$$\frac{R^2}{4L^2} < \frac{1}{LC} = \omega_o^2 \quad .$$

Then,

$$I(t) = \frac{V}{\omega L} \exp\left(-\frac{R}{2L}t\right) \sin\omega t \quad ,$$

where

$$\omega^2 = \omega_o^2 - \frac{R^2}{4L^2}$$

The peak current will be a maximum under these conditions, but the transfer of energy to the plasma will be small and the oscillatory nature of the discharge current will give rise to secondary bursts of plasma.

The other case of interest to us, because it gives the fastest non-oscillatory solution, is the one in which the circuit is critically damped. Critical damping occurs when

$$\frac{R_c^2}{4L^2} = \frac{1}{LC} \quad ,$$

that is when $R_c^2 = 4L/C$ the solution is then given by

$$I(t) = \frac{V}{L}\, t \exp\left(-\frac{R}{2L}\, t\right) \quad .$$

The overdamped case is of little interest because the pulses are longer in time and the peak current and energy transfer are reduced. Furthermore, if the external circuit resistance is small this condition is difficult to obtain. Let us compare the peak current, peaking time and initial current rise-rate for the two cases of interest. We use here values of circuit parameters from our apparatus, which are tabulated in Table 1.

Table 1

VALUES OF CIRCUIT PARAMETERS

Parameter	Value
Capacitance C	0.20 μf
Inductance L	0.507 μh
Natural frequency ω_o	500 kc/s
Internal resistance r	0.34 ohms
Surge resistance R_s	1.59 ohms
Critically damping resistance R_c	3.18 ohms

We have calculated from the measured frequency (500 kc/s), the inductance assuming zero damping. The internal resistance was calculated from the decay rate of the free oscillation. This is not exactly consistent, but introduces only small errors. A comparison of the calculated peak currents for the damped and undamped cases is shown in Table 2 for a typical value of initial condensor voltage, V equal 10 kilovolts.

Table 2

COMPARISON OF DAMPED AND UNDAMPED DISCHARGES (ACTUAL VALUES)

Parameter	Oscillatory	Damped
Resistance R	0.34 ohms	3.18 ohms
Peak Current I_m	6.55×10^3 amp	2.3×10^3 amp
Peaking Time t_m	0.441 μsec	0.38 μsec
Initial rate $(\frac{dI}{dt_o})$ of rise	1.97×10^{10} amp/sec	1.97×10^{10} amp/sec

What is not shown in the tables is the half-height width of the pulse and the related efficiency. The undamped circuit produces plasma over a shorter period of time, and hence one that is shorter in space. There can be no valid comparison of efficiencies for these two cases when the damping is affected by inserting external resistance. To efficiently critically damp the circuit one should add capacitance. This will generally increase the total inductance and resistance slightly, but will lead to the highest values of peak current. Gabriel, et al[8] gives a good discussion of high speed capacitor banks.

The stored energy varies as V^2, but to a zero order approximation, the power delivered to the arc varies directly as V (this assumes constant arc resistance and neglects dL/dt terms). It is also to be noted that at the lower pressures the amplitude and frequency of the discharge are completely controlled by the external circuit, and no measurable changes are seen in the discharge current when the arc is replaced by a heavy copper strap.

ELECTRODE EFFECTS

The plasma is produced by erosion of the electrodes, and one must be concerned with electrode reactions if overall efficiency is to be considered. As will be shown below the mass of material accelerated greatly affects the efficiency. It is apparent that if a finite energy is available from the storage capacitors, there is bound to be some optimum distribution between plasma

production and acceleration, if one desires the most energetic plasmoid. In our experiments there was no possibility of control over this distribution.

The details of the processes in the arc discharge depend on the class of electrode materials and the arc length. The distinction in electrodes is between cold cathode and ordinary arcs. Essentially the temperature is the same in each of these. The ordinary type implies a material that can supply the required arc current through thermionic emission at reasonable temperatures. This includes all the more refractory metals such as tungsten and molybdenum. In the cold cathode types the temperature is limited by boiling of the electrodes, and the arc current is not supplied by thermionic emission only. This includes such materials as copper, aluminum and mercury. Arc processes have been studied for many years, but are still not completely understood. Especially the cold cathode arc, which is the case for our copper electrodes. The processes at the electrodes include, electron emission (both thermionic and high field, and possibly photoemission and emission due to bombardment by excited ions), ion production, vaporization, heat transfer by radiation and conduction, and possibly optical radiation effects, such as excitation of ions. For this application we are interested mainly in the vaporization of the electrodes, and also with ohmic losses in the arc channel and electrodes. High velocity vapor jets have been observed[9] at arc electrodes, and they may be responsible for some of the energy of the plasmoid. Lee[10-14] and others[15-17] have recently made an attempt at a consistent theory for steady state arcs that suggests an approach for the transient case. Llewellyn[18] has made some attempt at a transient solution.

In the steady state one assumes thermodynamic equilibrium and balances the various heat inputs and losses. For a material like copper the radiation and conduction turn out to be rather negligible, and so does the electrode heating due to ohmic losses. The electron and ion current bombardment provides the main input and vaporization of the electrodes provides the output. The mass rate of evaporation may be calculated from the data given by Dushman,[19] and Kubachewski and Evans.[20] For the transient case, heat loss due to conduction may not be negligible.

If the power input due to ion bombardment is too great for conduction and radiation to dissipate the heat the electrode will evaporate (boil) at the surface and this will provide the major cooling effect. Because of this rapid erosion (ablation) of the surface the mass of material beneath the cathode spot may not be important in the calculation of temperature. The problem may be treated as a surface phenomena. Llewellyn[18] has made some attempt at this problem and obtained the following expression for the temperature rise. If $(r^2/kt)^{1/2} \gg 1$ and

$r \approx 10^{-3}$ cm then

$$\theta = \frac{2 Q t^{1/2}}{(\pi \lambda s \rho)^{1/2}} \quad ,$$

where s = specific heat
ρ = density
λ = thermal conductivity
$k = \lambda / s\rho$
t = time
θ = temperature rise
r = radius of cathode spot
Q = power input density

These conditions hold true for the copper electrodes in our experiment and a typical time to reach the boiling point of copper (2570°C) is about 10^{-8} seconds. This is short compared to our pulse length, so the process is essentially limited by vaporization. This also indicates that, except for the shortest times, we may consider the processes as quasi-steady state (see also Lee[14]).

This analytical approach has limited applicability because of the breakup of the cathode spot when high currents are carried. The photographs of the electrodes show the multiplicity of cathode spots. This is in agreement with the literature,[21] where multiple spots are known to form for currents of 2-10 amperes. The current density at each spot appears to be high (10^6 amp/cm^2) and constant from spot to spot. Lee[14] discusses the hydromagnetic forces on the arc channel and the possibility of self pinch off. This does not seem to occur in our experiment. This phenomena would result in discontinuities in the discharge current as in the case of a. c. arcs that extinguish before zero current is reached. This would seem to eliminate any pinch mechanisms as the accelerating force, which had been tentatively suggested by Finkelstein et al.[22] In general, one suspects that pinch forces produce no net momentum.

Because we had intended to estimate the amount of material eroded during a single discharge by studying the size of the craters, photographs were taken of the electrodes. Although we knew of the formation of multiple cathode spots, we did not really expect the results obtained here (see Figures 3-5). Other measurements of material erosion from electrodes have been made.[23, 24] The values reported range from 7-87 gm/coul. For a typical case in our experiment this would indicate a total mass of evaporated material of $52.5 - 435 \times 10^{-9}$ grams/discharge. With a velocity of 5×10^6 cm/sec this indicates a total kinetic energy of about 3.75×10^6 gm. cm^3/sec^2. This is probably too large for our plasmoids, since much of the material eroded seems to come off as large pieces which move in straight lines through the field and do not stay with the main plasmoid. This is deduced from photographs where many straight bright tracks emenate from the source.

There still remains the possibility of making an engineering guess about the relative production efficiencies of various materials. Consider two commonly used materials, copper and tungsten. To make the comparison we assume that both materials operate with the same current density and cathode drop, although actual values could be put in if they were known. We also neglect radiation and conduction losses, this can generally be justified because the rapid ablation of the surface allows us to treat the problem as a surface phenomenon.

The main source of cooling will be evaporation of the metal. The latent heat of evaporation of tungsten is 11.5 joules/gram, and that of copper is only 5 joules/gram. If this were the only cooling source we would expect to evaporate one-half as much tungsten as copper. For tungsten there is an additional heat loss due to electron evaporation of $nJ\phi$, where n is the fraction of current carried by the electrons, and ϕ is the work function. For copper where the electron emission is due to high field effects we do not have this cooling effect because the electrons come from the fermi level without being thermally excited. This will provide a further small advantage to copper. In general the low melting point metals with low latent heats of evaporation will have the highest production efficiencies. The low melting point limits the thermionic emission, and the low latent heat demands greater masses of material to balance the heat input. One might then formulate an expression that involves the cathode drop, latent heat of evaporation, and thermal diffusivity to account for transient thermal conduction effects. This would give an indication of a best material although ionization efficiencies are important in that only the ions (and electrons) can subsequently be accelerated.

ACCELERATION OF PLASMOID

The acceleration is caused by the interaction of the current with the electrodes through the medium of the magnetic field, but analysis of this phenomena is in the present case very difficult. If one considers more amenable geometries, then some approach to the problem can be made. This has been done by various authors under several different assumptions. The rail accelerators were analyzed by Bostick assuming that the slug of plasma did not spread, but accelerated as a whole, and that certain resistances are negligible. Thourson[25] has taken these results and done an analog computer study for 12 cases. There are other more general analyses available Mostov et al,[26] and Steckly.[27] The usefulness of these mathematical manipulations is either to aid one in understanding the interactions of the parameters in a general way or to compare various geometries at least under idealized conditions. We do not believe that they can have much meaning when applied to the button source.

PLASMA MOTION

The problem of the plasmoid motion through a magnetic field is complex and we don't have a complete solution. Zadoff et al[28] has shown that

a plasma cannot be self containing in more then two directions and has discussed the expansion for a special case. We know that without a background field we do not get plasmoid formation, but get instead an isotropic burst of plasma that rapidly dissipates. It apparently, however, reaches the opposite wall of the chamber, for probe measurements indicate a rapid propagation of some ionized material, but without a luminous trail.

Bostick's group has shown that instabilities apparently occur[29, 30] when the plasmoid moves into a region of non-uniform field. The field in the region of the source during the initial discharge is extremely non-uniform and this may be the explanation to the formation of the plasmoid. Once the plasmoid has been given its initial acceleration by the various magnetic pressures, it should stay together for a fairly long time. The internal temperature seems to be rather low in comparison to the directed kinetic energy (e. g., 100 ev compared to 3, 000 ev). Thus in the short flight time of the plasmoid, the lateral spread due to thermal effects would be small. The axial spread is not inhibited and seems to be controlled by the acceleration forces and not the temperature. Measurements indicate that the velocity along the magnetic field lines is of the same order as that in the main direction of motion.

We suggest the following assumptions to explain the plasmoid motion:

1. The acceleration is due essentially to the reaction of the electrodes on the arc caused by the magnetic field.

2. Plasmoid formation occurs because of some instability mechanism as the plasma expands into the background field, which causes a channeling of the plasma.

3. The result of the initial production and acceleration is a low density plasma moving through a magnetic field which tends to impede its motion.

4. The internal temperature is low and hence the relatively small expansion as the plasma moves through the field.

One might attempt a solution to the problem of the expanding plasma bubble in a magnetic field, but a great many assumptions would have to be made. We have used an experimental approach to the problem using photographic techniques and velocity measurements to get at least a basic understanding of the mechanisms involved.

PROBE MEASUREMENTS OF VELOCITY

The velocity and, somewhat more important, the acceleration of the plasmoid are quantities that must be measured and known to understand the generation mechanism. However, because of the high velocity and somewhat unstable nature of the plasmoid these measurements are rather difficult to make. A simple way to measure the velocity is by means of photomultiplier telescopes. Two or more photomultipliers with lenses and appropriate slits

to limit the viewing area, are placed at known distances along the path of the plasmoid. Signals from the photomultipliers as recorded with an oscilloscope and camera give the velocity and apparent length of the plasmoid. We are not able to utilize this method too effectively in our experiments because of the relatively small chamber size, which was limited by the difficulty of producing a uniform magnetic field over a large volume.

We have used a method that is also simple and is more applicable to our equipment. It involves a probe whose position along the plasmoid course is varied to obtain time of arrival differences. Because a series of measurements must be made to obtain a single velocity profile, we are actually measuring the average velocity of a group of plasmoids. A relatively large number of measurements were made at each point and the close grouping of the data indicates that the velocity obtained is really indicative of the individual plasmoid. We also measured the velocity with a high speed electronic camera, and although these measurements are not precise, they do agree with about 30 percent error. It has been reported that velocity measurements based on the luminous front and the ionized front do not agree (Clauser[31], p. 284); however, our measurements are not precise enough to allow us to resolve this question.

The probe design is not critical. A short length of wire mutually perpendicular to the directions of the magnetic field and the motion of the plasmoid will suffice. The connecting wire is insulated and sealed through a vacuum connection (see Figure 6). The probe calibrated in centimeters with the zero point about 3 cm from the source. This is far enough away to observe the plasmoid free of its source. Since it was difficult to position the probe exactly, measurements for a range of magnetic field and capacitor energy were made for each probe setting. A series of at least three measurements were made for each value of field and discharge voltage at each position. Many series of measurements were made and they all agree very well. It is difficult to plot these all together because of the error in the absolute probe position.

The results of the measurements are presented in Figures 8 and 9. Note that the highest velocity occurs when there is no background field. For the cases with the magnetic field, the highest velocity occurs when the background field is parallel to the self-field of the discharge arc loop. Professor Bostick[2] has made velocity measurements with a background field perpendicular to the self-field. The velocity for this case falls between the values for the parallel and anti-parallel cases. The overall indication is then that the magnetic field exerts a drag on the plasmoid during its free flight, but depending on its relative orientation either increases or decreases the initial acceleration. The velocity appears to be a constant over the measured range of 10 cm, so that while the effect of the field is to retard the plasmoid it either does not exert a constant force, (which would require a diminishing velocity), or the chamber is not large enough to allow us to observe this effect.

PHOTOGRAPHIC MEASUREMENTS

Using the image converter camera described below, we took a series of photographs of the flight of the plasmoid. The synchronization problems were solved by the electronic switching of the discharge, and all times are with respect to the initiation of the discharge. Because it is difficult to know where the plasmoid is going to be in the chamber at any given time, the magnification ratio was adjusted so that the entire 20-cm diameter vacuum chamber was imaged onto the 2-cm diameter photocathode of the image tube. The pressure in the plasmoid chamber during all these tests was less than 10^{-5} torr.

The exposure was always set at the minimum time commensurate with the light level available. An exposure time of 0.2 microseconds was a good average, for it enables us to follow the plasmoid half way across the chamber. Longer times were required to follow the plasmoid at later times. With a velocity of 5 cm/microsecond the plasmoid moves 1 cm in 0.2 microseconds, and at longer exposures the blur becomes excessive. Even at longer exposures where the total movement is large, some degree of sense can be made from the photos. Here the central portion of the plasma trace will be brightened by overlap of the exposure. There are three series of photographs included in the figures shown:

I.	Figures 10-15: 0.2 μs exposure	0.5 μs interval
II.	Figures 16-18: 0.5 μs exposure	1.0 μs interval
III.	Figures 19-22: 2.0 μs exposure	Various intervals.

All of these photographs were originally made on polaroid film and copied to provide enlargements. The overall enlargement factor was held constant for each series.

To interpret these photographs we must consider the sequence of events. The time delay is measured with respect to the initiation of the discharge current, which follows an almost critically damped sinusoid that decays to zero in 2.0 microseconds. The bright spot at the upper right is the intense glow around the actual discharge. We see that this glow persists for at least 3 microseconds after the discharge current has decayed to zero (see Figure 15). The bright streak moving away from the source is caused by either emission from the actual plasma material or from collision of the plasma with the background gases. It is difficult to determine where the light originates, and a spectrographic study would be required to make a final decision.* Comparing the three sets of photographs, we see that figures 19-22 are characterized by uniformly bright streaks (the plasma moves a distance of 10 cm during the exposure) with very little detail apparent; however, the plasma seems to disconnect from the source leaving a dark space. In the other figures there is less movement during the exposure, but even with 0.2 microseconds exposure (Figures 10-15, the

---

*The source of light has not been resolved, and is probably dependent on the pressure regime in which one operates. See the remarks by Kolb and Bostick in Ref. 31, p. 284.

image grows in length as time progresses with the front moving faster than the rear. This may be caused either by the velocity spread of the plasma, where the slower material falls behind the main body (notice the bright central spot in figures 13 and 17), or by a luminous wake left in the background.

There is a lack of detail in all the photographs due in part to the resolution of the camera and in part to the plasmoid motion during the exposure. From these photos we cannot decide the question of structure. The evidence from both the photographs and probes indicates an amorphous jet rather than a detailed structure. It would have been interesting to take more photographs with the shortest possible exposure and, if possible, to coordinate these with probe measurements.

In addition to the high speed photographs we have taken many time-integrated photographs with either 35 mm or Polaroid Land cameras, which were useful in checking the interaction of the plasmoid with the probes. Many of these pictures are interesting in their own right (see Figures 23-28). There is a distinct difference between plasmoids formed when the discharge magnetic field is parallel to the background magnetic field (positive field sense) and those formed when the fields are anti-parallel (negative field sense). We have already seen the difference in velocities for the two cases. The acceleration is caused by the interaction between the arc current and the total magnetic field. The effects of the background field are twofold. One, it either aids or hinders the acceleration during the plasmoid formation period, and, two it provides a background medium for the plasma to move through after the acceleration period. The discharge field must be a good deal stronger than the background field, because the arc loop always expands and the plasmoid is always accelerated away from the source. However, the background field provides the essential difference between the two cases. When the field is in the negative sense the luminous trajectory of the plasmoid is a narrow bright stripe. When the field is positive the picture shows a broader diffuse plasmoid often split into two separate sections (see Figure 24). In many of the pictures (see Figure 26) the two halves remain separate until they strike the wall. This would tend to support the theory that the plasma comes off as two separate jets, one at each electrode (c. f. Finkelstein et al reference 22). The positive field always has an outward directed force on the arc loop, but the negative field may have an inward force during the early stages of formation that compresses the arc channel before it is accelerated away (see Figure 29). It is interesting to note that the plasmoids formed in the negative sense fields seem to be much "stiffer" as evidenced by their interaction with small obstacles (a thin wire probe). Some of the apparent interaction with the wire is caused by a discharge current that occurred when the plasmoid reached the wire. This was later corrected by revising the grounding arrangement on the probe.

EXPERIMENTS WITH THE DUAL PLASMOID SOURCE

Because of the high velocities with which the plasmoids travel, and because of the difficulties in trying to measure their characteristics by

means of probes which are a perturbing influence, people have tried to use the interaction of two or more plasmoids as a diagnostic tool. However, if two plasmoids collide the resulting interaction is difficult to interpret.

We felt that a less dramatic interaction would be more edifying. This resulted in our experiments with the dual plasmoid source. This was a button gun with two sets of wires that produced two plasmoids (see Figures 30 and 31), which were propelled on initially parallel paths. Notice that whenever divergence occurred the field was in the negative sense. However negative fields did not always produce divergence, which proved to be a rare phenomena. This may be seen in Figure 33f which is a photo of two diverging plasmoids. Figures 32 and 33 show the effects of field strength and direction on the interaction. These samples were chosen to be representative, except for the divergent case which was rare and not reproducible.

Our initial experiments gave a decided result. The two plasmoids could be made to converge or diverge depending on the field strength and direction. This seemed promising and a tentative theory was outlined and reported.* Unfortunately, these results could not be repeated and these ideas had to be discarded. The negative results lead one to believe either the plasmoids have very little magnetic moment and/or electrostatic dipole moment or that the total interaction time is too short to produce a measurable effect.

THE EXPERIMENTAL APPARATUS

We shall describe below in some detail the experimental apparatus, including the electronic equipment for the image converter camera. The apparatus consists of a vacuum system, a large magnetic field system, the plasmoid generator, and the diagnostic equipment. The vacuum system is of course independent, but the other equipment is all interconnected. The overall concept can be seen in the block diagram (see Figure 34), and an overall view of the apparatus in figure 35 (this is an older photo and does not show the ignitron switch). Synchronization of these interconnected events is the major requirement of the equipment. If reproducible results are to be obtained the jitter in the switches must be kept to a minimum.

The sequence is initiated by a manual push button that triggers the spark gap switch for the magnetic field. To eliminate the jitter in this switch we generate the next trigger signal from the initial rise of the magnetic field. This trigger is delayed to permit choosing the magnetic field strength as explained below. This delayed trigger is fed simultaneously to the plasmoid generator and camera. The plasmoid generator has an intrinsic delay of 4 microseconds and the camera has an adjustable delay of 1-100 microseconds so the camera can be opened before the plasmoid is generated. The jitter in these circuits is very small and has been barely detectable in our measurements; however, we monitor the plasmoid current pulse and camera "on pulse" so as to always have an exact measurement of the time relation.

---

*D. DeGeeter, Bull. Am. Phys. Soc., V5, p. 413, abstract F5.

The vacuum system will not be discussed in detail as it is completely ordinary and uses standard components. Various views of this system can be seen in Figures 36, 37 and 38. The measurement chamber is a glass cylinder with four viewing ports. The cover end rests on a rubber gasket and the upper end is closed with a flat glass plate and an O-ring. The various side ports through which the plasmoid source or various probes are inserted are sealed with either a brass cap held with a vinyl seal or with a plastic disc and an O-ring. The pumping equipment consists of a liquid nitrogen cold trap, a 4-inch mercury diffusion pump and a standard backing pump. The ultimate pressure obtainable was 3×10^{-6} mm of Hg which, considering all the O-rings and other seals is quite good.

THE MAGNETIC FIELD SYSTEM

The magnetic field in the measurement chamber is produced by the discharge of a bank of capacitors through a large single layer solenoid. The solenoid consists of approximately 100 turns of number 2 copper wire. The coil is 12 inches in diameter and 30 inches long. The wire was wound on a wooden form and then embedded in epoxy resin for insulation and mechanical strength. The turn spacing and the length to diameter ratio are such that the field is quite uniform in the central region where the plasmoids are formed. The coil fits over the vacuum chamber, and four viewing ports have been made in the coil.

The capacitor bank consists of four John Fast 175-microfarad capacitors in parallel for a total of 700 microfarads. The capacitors are standard a. c. line capacitors rated at 4,000 volts, and were normally charged to 3,000 volts. The capacitors are connected to the large coil by a triggered gap and heavy copper bus bar which can be seen in Figure 36. The gap is of simple design consisting of two 1-inch diameter copper rods faced with molybdenum to reduce erosion. The gap is spaced to hold off about 3,200 volts and is triggered by a 10 -kilovoltpulse to a wire which projects into the gap. The schematic diagram for the pulse generator may be seen in Figure 40. This gap switch (Figure 39) has a rather high jitter and tends to be somewhat erratic in its behavior. However, this does not affect the rest of the sequence because the trigger for the plasmoid generator is derived from the initial rise of the magnetic field.

The discharge oscillates with a period of 6 milliseconds. The variation of the field during the 6-microsecond lifetime of the plasmoid is negligible and the field may be considered constant. The main reason for using a capacitor discharge to generate the field is convenience in obtaining high currents; however, there are additional benefits. The decay of the circuit is small so the second half cycle amplitude is 90 percent of the first. By delaying the generation of the plasmoid we can chose any value of magnetic field between $\pm B_{max}$. This is especially convenient when triggered gaps are used because they do not lend themselves to operation over a wide voltage range and it would be inconvenient to change the field strength by changing the voltage on the capacitors. The magnitude field was measured with a search coil and found to be very uniform over the cross-sectional area of the solenoid. A calibration measurement gave the following expected

value for the peak magnetic field strength at 3000 and 4000 volts on the capacitors: 4100 $\pm$ 200 and 5300 $\pm$ 300 gauss, respectively.

THE PLASMOID GENERATOR

The plasmoid is generated by means of a transient high current arc across two wires in a configuration generally called the Bostick button source. The two wires run parallel up the plastic or glass tube and are imbedded in epoxy resin for insulation and mechanical strength. For a typical design with 10 kiloamperes peak there is a peak force separating the wire of 1,000 lbs/cm. This causes a peak tensile stress of approximately 10,000 lbs/cm^2 in the epoxy resin and many of the sources develop strain cracks after repeated use. We have generally used copper wire, but some of the earlier experiments were done with hydrogen loaded titanium wire. No special precautions were used in constructing these sources and they all performed about the same. It is interesting to note that when the wires were micropolished for a special test, we experienced great difficulty in that the gap would not break down. Earlier tests had shown that about 3,000 volts were required to break down the gap. This was obviously greatly increased by the polishing. A soft lead pencil may be used to provide a conducting path between the electrodes to provide a more uniform breakdown.

The current for the discharge is obtained by discharging another capacitor. The characteristics of this discharge were discussed in Part I of this report. A small value of capacitance and inductance is required for a high speed discharge, so high voltages are required to attain reasonable energies. The original apparatus used a 0.02 -μf 50-kv capacitor. This gave a natural frequency of 1.2 Mc/s. A three-ball gap (as seen in Figure 35) was used as a switch. This had excessive jitter, poor reliability and limited voltage range (without adjusting the spacing); in addition, it was difficult to generate a fast rise-time trigger pulse with the required amplitude (15 kv). To eliminate these difficulties the equipment was modified to use a G. E. type 7703 ignitron. This special tube for capacitor switching service is rated at 100 kiloamperes and 20 kilovolts. The capacitance was increased to 0.20 microfarads partially to compensate for the reduced voltage rating and partially because we desired a greater storage capacity. With the normally used voltage of 15 kv this system has a rating of approximately 30 joules. The installation of the ignitron to replace the 3-ball gap may be seen in Figure 41. We have used heavy copper bus bar, arranged to minimize the inductance, and enclosed in polystyrene for insulation and mechanical rigidity.

The pulse circuitry is very straightforward. The system has performed well and no modifications are suggested. The circuit is shown in Figure 42. The trigger for this circuit is obtained from 2D21 thyratron triggered by the 0-5 millisecond delay generator. This same trigger is also fed through a delay generator to the camera gate generator. The overall delay of the camera circuits was greater than that of the plasmoid circuits, so a delay line was inserted into the plasmoid circuit to permit the camera to photograph the initiation of the arc.

One other important part of the plasmoid generator is the current measuring resistor. The requirements of such a resistor are that its resistance be small compared to the load resistance and that it have low inductance. Because of the high currents there are also mechanical and thermal stress considerations. Also because of the high currents it is better if one end of the resistor can be grounded without introducing extraneous voltages. We experimented with various shunts designed to have low inductance; however, most of these did not perform satisfactorily and gave distorted waveforms and indicated low values for the peak current. We are presently using a coaxial shunt as described and analysed by Park.[32] Our design may be seen in Figure 43. This shunt has a calculated resistance of 0.9 of the d.c. resistance at a frequency of 500 kc/sec. The measured values of current when connected for this agree very well with the theoretical value and the shunt is considered satisfactory.

THE IMAGE CONVERTER CAMERA

A high speed camera has been built around an RCA type C73435B (developmental type designation) image converter tube. These tubes were originally designed as frequency converters, but recently have been redesigned for use as fast shutters.[33,34] Until very recently no commercial cameras using these devices were available, and we therefore constructed our own. The conception and construction of this camera is very simple and no sophisticated techniques have been used (c.f. see Richards, reference 50 for a discussion of a more elaborate design). This has led possibly to some degradation in performance from the theoretical expectation, but this is somewhat a matter of the care used in setting the camera up. We had a chance to compare our camera to a commercial* unit during a trial demonstration. The trial was not completely successful, so a really fair comparison cannot be made. However, in our judgment our camera was more convenient to use and had as good or better resolution and image brightness.

The complete camera unit consists of a Sonnar F/15, 125-mm focal length objective lens, the electronic shutter and a polaroid back camera with an f 1.2 lens. With polaroid 3000 ASA rating film this provides an extremely fast system usable to exposure times of 50 nanoseconds. The image tube is a triode and incorporates deflection plates permitting its use as a framing or streak camera. The S-11 photocathode and the P-11 phosphor have approximately the same frequency response peaking in the visible spectrum. The manufacturer claims a light gain of 24 at the peak of the spectral response at 4,400 A. Other pertinent data on the tube is available from RCA Electron Tube Division, Harrison, New Jersey

One advantage of the triode tube is that one does not need fast-rise and fast-decay high-voltage pulses. However, the focus of the tube is a function of the tube voltages and relatively precise amplitudes are required. We have eliminated the need for fast decay pulses by using two fast-rise steps: one applied to the cathode turns the tube on and one to the grid turns it off. These pulses are negative because it is usually easier to generate

---

* Abtronics, Inc., 63 South P Street, Livermore, California.

a fast negative pulse. The operation is simple and is indicated in the block diagram Figure 44. The ultor voltage is fixed at 15 kv, the maximum allowable. The grid-cathode and first anode voltages must be adjusted to eliminate the shadows of the grid wires and to give the best focus with maximum field flatness. These adjustments interact, and the proper values are generally found for continuous operation and then the pulse voltages are adjusted to these values.

In actual operation the cathode is biased positively to cut off the tube and the gate is negative. The amplitude of the on-gate is adjusted for best focus, but the grid-cathode bias may also be used to focus the camera, as long as it is greater than the value required to keep the tube cut off. The exposure time is set by delaying the trigger to the off gate. At present a 0-3 microsecond delay line is used but this could be increased. The lower limit on exposure time is set by the rise time of the gate which is 10 nanoseconds. This limits the minimum exposure to approximately 50 nanoseconds, but improved design could lower this if desired. Low light intensity has limited us to a minimum exposure of 100 nanoseconds. The tube itself is only rated for a minimum of 100 nanoseconds and the resolution may be poor below this although the tube still works. The upper limit on exposure time is set by the flatness of the gate pulse. The on-gate pulse drops quite rapidly and the present limit is probably 10 microseconds. This could also be improved with some slight redesign.

An overall view of the camera may be seen in Figure 45. The power supplies are in the relay rack; the gate generators, trigger and delay line are the camera chasis. The image tube itself may be separated from the chassis, although the rise time of the gate pulse will be increased if the cables are lengthened. Standard power supplies may be used, but some method of over voltage protection should be used. The camera circuits are shown in Figures 46 and 47. A useful modification for this camera would be a balanced deflection circuit permitting its use as a streak camera. About 1000-volt peak to peak would be required and a rundown time of 5 microseconds would be satisfactory although it should be adjustable.

REFERENCES

1. Bostick, W. H., "Experimental Study of Plasmoids", Phys. Rev. 106, 404-412, 1957.

2. Bostick, W. H., Harris, E. G., Theus, R. B., "Experimental Investigations of the Motion of a Plasma Projected from a Button Source Across Magnetic Fields", Phys. Rev. 105, 46-50, 1957.

3. Bostick, W. H., "Experimental Study of Ionized Matter Projected Across a Magnetic Field", Phys. Rev. 104, 292-299, 1956.

4. Morozov, A. I., "The Acceleration of a Plasma by a Magnetic Field", Soviet Physics - JETP 5, 215, 1957.

5. Plyutto, A. A., "Acceleration of Positive Ions in Expansion of the Plasma in a Vacuum", Soviet Physics - JETP 12, 1106, 1961.

6. Raab, B., Experimental Research on Expanding Plasmas and Plasmoids, AFSWC-TR-59-65, November 1959.

7. Kash, Sidney W., "Efficiency Considerations in Electrical Propulsion", Plasma Acceleration, S. Kash, ed., Stanford, 1960.

8. Gabriel, H., Howell, V., Thorton, E., Wilson, R., Low Inductance Capacitor Banks and Linear Pinched Discharges", Jour. Sci. Inst. 38, 136, 1961.

9. Finkelnberg, Wolfgang, "A Theory of the Production of Electrode Vapor Jets by Sparks and Arcs", Phys. Rev. 74, 1475, 1948.

10. Lee, T. H., "On the Mechanism of Electron Emission in Arcs with Low Boiling Point Cathodes", Jour. Appl. Phys. 28, 920, 1957.

11. Lee, T. H., "On the Discussion of T-F Theory by Robson and Von Engel", Jour. Appl. Phys. 29, 734, 1958.

12. Lee, T. H., "T-F Theory of Electron Emission in High-Current Arcs", Jour. Appl. Phys. 30, 166, 1959.

13. Lee, T. H., "Energy Distribution and Cooling Effect of Electrons Emitted from an Arc Cathode", Jour. Appl. Phys. 31, 928, 1960.

14. Lee, T. H., Greenwood, Allan, "Theory for the Cathode Mechanism in Metal Vapor Arcs", Jour. Appl. Phys. 32, 916, 1961.

15. Von Engel, A., Robson, A. E., "Mechanism of Electrode Emission from the Arc Cathode", Jour. Appl. Phys. 29, 7342, 1958.

16. Von Engel, A., Robson, A. E., "Excitation Theory of Arcs with Evaporating Cathodes", Proc. Royal Soc. A243, 217, 1957.

17. Von Engel, A. and Arnold, K. W., "Step Wise Ablation and Heat Transfer in Cold Cathode Arcs", Nature, 187, 1101 (L), 1960.

18. Llewellyn Jones, F., The Physics of Electrical Contacts, Oxford, 1957.

19. Dushman, S., Vacuum Technique, Wiley, 1949, 3rd printing.

20. Kubaschewski, O., Evans, E., Metallurgical Thermochemistry, Pergamon Press, 1958.

21. Somerville, J., Blevin, W. R., Fletcher, N. H., "Electrode Phenomena in Transient Arcs", Phys. Soc. Proc. B65, 963, 1952.

22. Finkelstein, D., Sawyer, G. A., Stratton, T. F., "Supersonic Motion of Vacuum Spark Plasmas Along Magnetic Field Lines", Phys. Fluids 1, 188, 1958.

23. Tannerberg, R., "On the Cathode of an Arc Drawn in Vacuum", Phys. Rev. 35, 1080, 1930.

24. Corbine, James D., Gaseous Conductors, Dover, 1958.

25. Thourson, Thomas L., "Pulsed Plasma Accelerator", Second Symposium on Advanced Propulsion Concepts ARDC-AVCO, 1959.

26. Mostov, P. A., Neuringer, J. L., Rigney, D. S., "Electromagnetic Acceleration of a Plasma Slug", Phys. Fluids 4, 1097, 1961.

27. Steckly, Z. J. S., Analysis of Constant Velocity Pulsed Plasma Accelerator, Avco Research Report 89, 1960.

28. Zadoff, L. N., Berstein, M., Reinheimer, J., Self Confinement of Plasmas, Republic Aviation Corp., MSD 206-995, 1959, AD 236-699.

29. Bostick, W. H., Dickinson, H., DiMarco, J. N., Kaslov, S., "Experimental Study of Explosions of High Temperature Plasma Perpendicular to a Magnetic Field and Resulting Rayleigh-Taylor Instabilities", Bull. APS 5, 342, 1960.

30. Dickinson, H., Bostick, W., DiMarco, J., Koslov, S., "Observations of Apparent Flute-Type Plasma Instability", Phys. Fluids 3, 480L, 1960.

31. Clauser, Milton U., The Magnetic Induction Plasma Engine, Space Technology Labs., TR 60-0000-00263, 1960.

32. Park, John H., "Shunts and Inductors for Surge-Current Measurements", Jour. Res. N.B.S. 39, 191, 1947.

33. Linden, R. B., Snell, P. A., "Shutter Image Converter Tubes", Proc. IRE 45, 513, 1957.

34. Stoudenheimer, R. G., Moor, J. C., "An Image-Converter Tube for High Speed Photographic Shutter Work", RCA Review 18, 322, 1957.

BIBLIOGRAPHY

PLASMOID AND PLASMA ACCELERATION

1. Andrew, Alan and Fitzpatrick, James, R., "Plasma Acceleration in a Vacuum", Bull. A. P.S., 5, 350, 1960.

2. Askarjan, G. A., "Acceleration of Charged Particle in Running or Standing Electromagnetic Waves", Soviet Physics - JETP 9, 430L, 1959.

3. Artsimovich, L. A., Lukianov, S., Podgoryi, I., Chuvatin, S., "Electrodynamic Acceleration of Plasma Bundles", Soviet Physics - JETP 6, 1-5, 1958.

4. Bostick, W. H., Nankivell, J., Koslov, S., "Experimental Studies on Plasma Dynamics", ARS-Northwestern Gas Dynamics Symposium, August, 1959.

5. Bostick, W. H., Byfield, H., Nankivell, J., "Measurements on the Efficiency and the Velocity Profile of a Coaxial Pulsed Plasma Motor", Bull. APS 5, 1960.

6. Clauser, Francis H., Symposium of Plasma Dynamics, Addison-Wesley, 1960.

7. Finkelstein, D., Wetstone, D. M., Ehrlich, M. P., "Experiments on Plasmoid Motion Along Magnetic Field", Phys. Fluids 3, 617, 1960.

8. Kvartskhava, I. F., Meladze, R. D., Suladze, K. V., "Experiments on Electrodynamical Acceleration of Plasmas," Soviet Physics - Tech. Phys. 266, 1961.

9. Miller, M. A., "Acceleration of Plasmoids by High Frequency Electric Fields", Soviet Physics - JETP 9, 1358, 1959.

ARCS AND PLASMA PRODUCTION

10. Corbine, J. D., Gallagher, C. J., "Current Density of the Arc Cathode Spot", Phys. Rev. 75, 1524, 1948.

11. Corbine, J. D., Burger, E. E., "Analysis of Electrode Phenomena in the High Current Arc", Jour. Appl. Phys. 26, 895, 1955.

12. Germer, L. H., Boyle, W. S., "Two Distinct Types of Short Arcs", Jour. Appl. Phys. 27, 32, 1956.

13. Hemqvist, K. G., "Emission Mechanism of Cold-Cathode Arcs", Phys. Rev. 109, 636, 1958.

14. Lutz, A., "The Cathode Phenomena of the Mercury Arc", Rev. Gen. Elec., 59, 159, 1950.

15. Zingerman, A. S., "On the Problem of the Metal Melted During Electrical Discharge Erosion", (In Russian), Fiz. Everdago Tela. 1, 284, 1959.

MEASUREMENTS AND EQUIPMENT

16. Chippendale, R. A., "Image Converter Techniques Applied to High Speed Photography", Photo. Jour. 92B, 149, 1952.

17. Jenkins, J. A., Chippendale, R. A., Philips Tech. Rev. 14, 213, 1953.

18. Hogan, A. W., "Use of Image Converter Tube for High-Speed Shutter Action", Proc. IRE 39, 268, 1951.

19. Richards, M. S., "An Instrument for the Observation of Very High Speed Phenomena", Proc. IRE 99, pt. 3, 729, 1952.

20. Turnoch, R. C., "Performance of Image Converters as High-Speed Shutters", Proc. IRE 98, pt. 2, 635, 1951.

Figure 1. Plasmoid Source

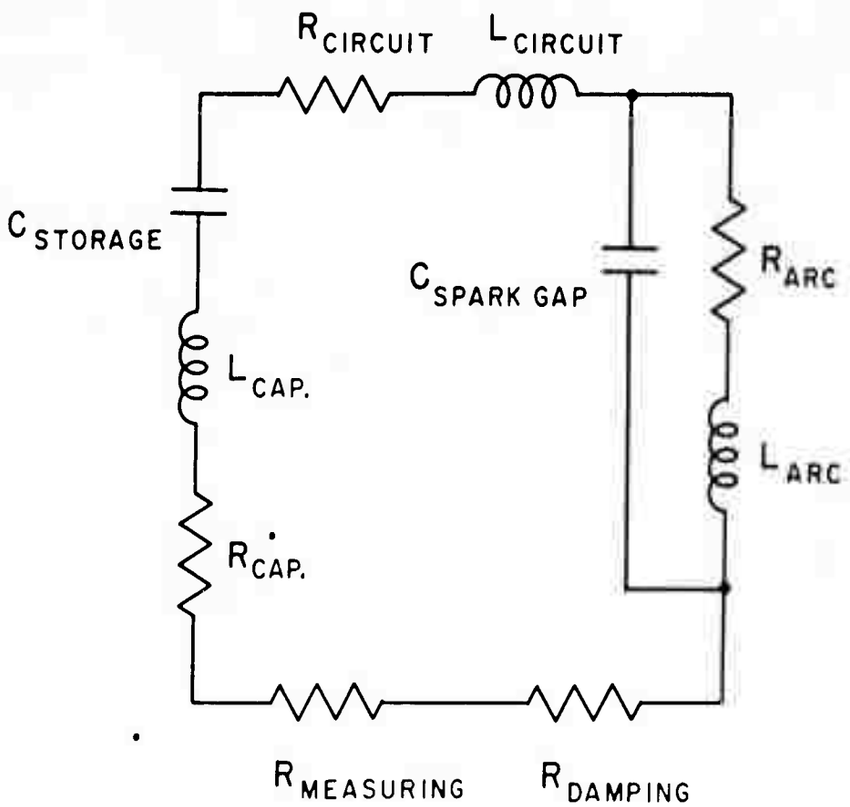

Figure 2. Idealized Discharge Circuit.

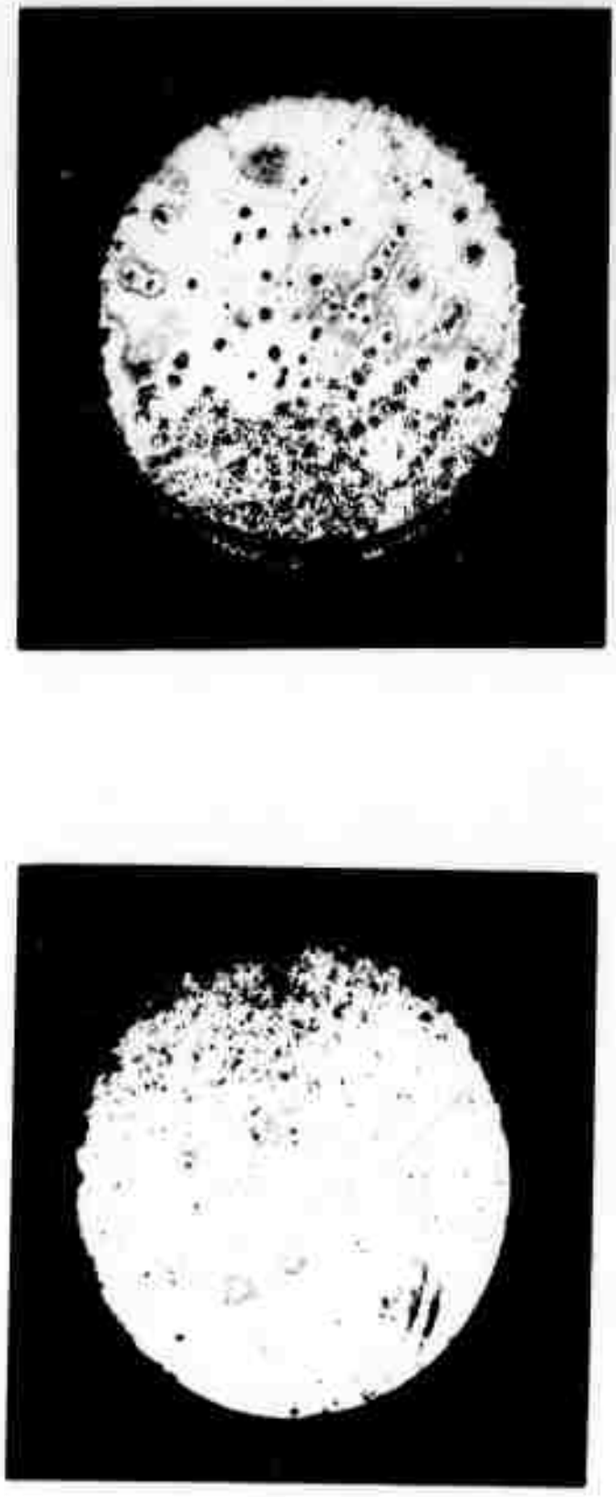

Figure 3. Microphotograph of Electrodes After a Single Discharge. Anode at Top - 50 x Magnification.

Figure 4. Microphotograph of Electrodes After 3 Discharges. Anode at Top - 50 x Magnification.

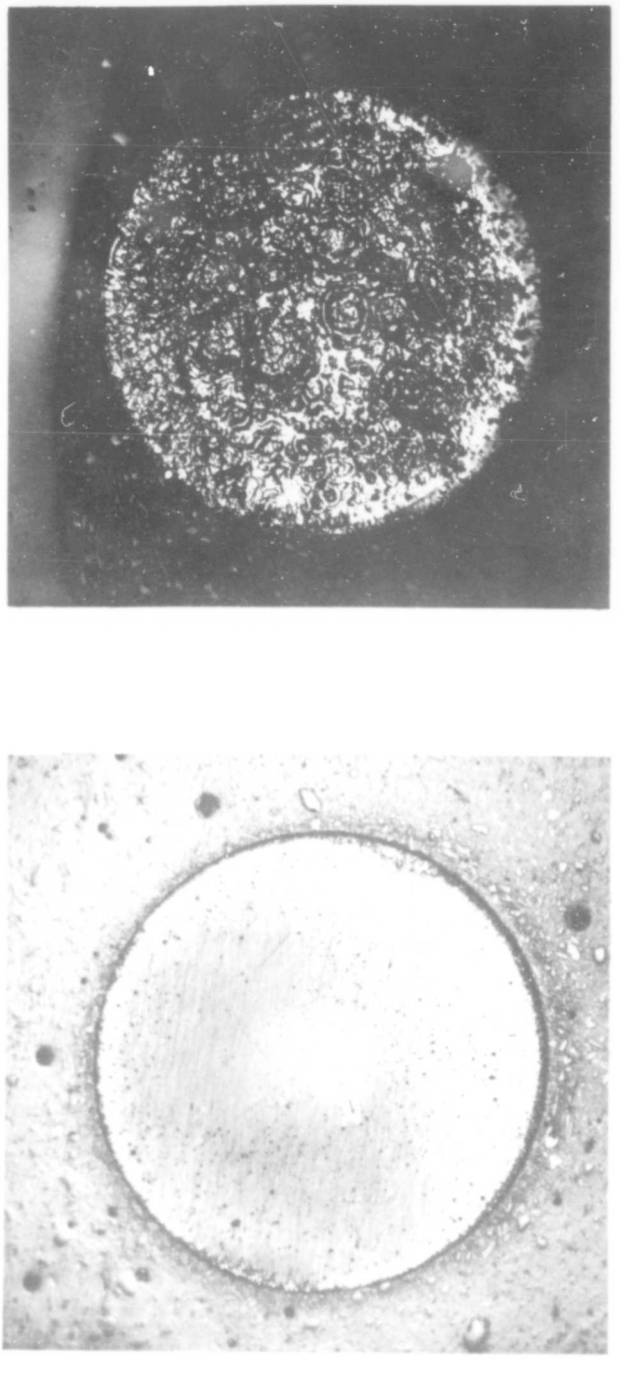

Figure 5. Microphotograph of Electrodes After Continuous Discharge. Anode at Top - 50 x Magnification.

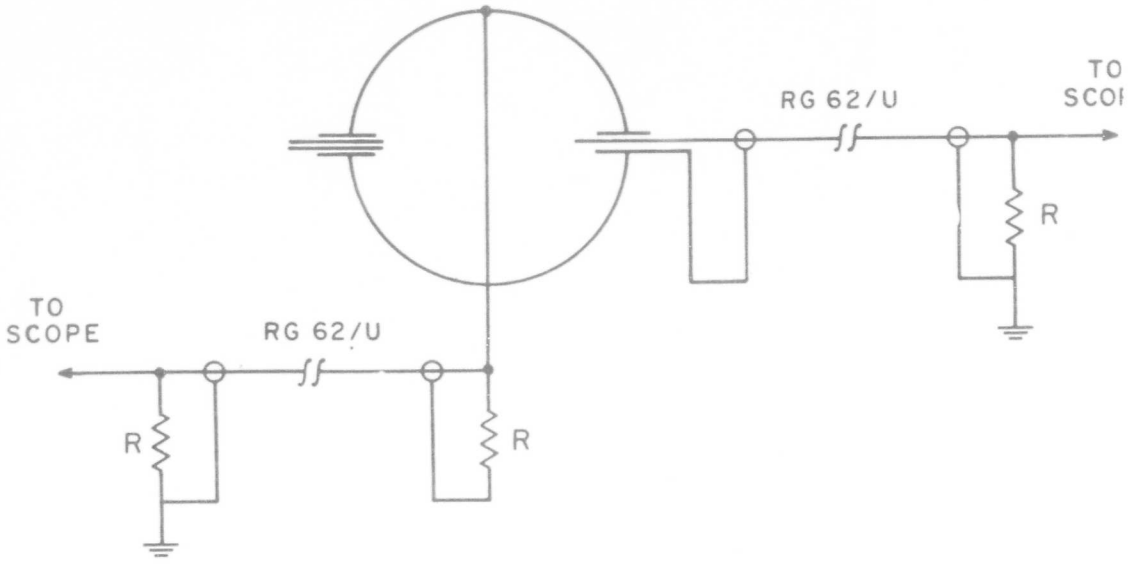

R IS A TERMINATING RESISTOR WHOSE VALUE WAS VARIED DURING THE TESTS

Figure 6. Schematic View of Probes

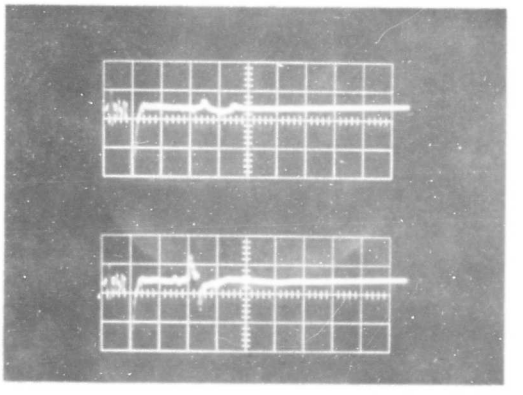

Figure 7. Typical Probe Trace

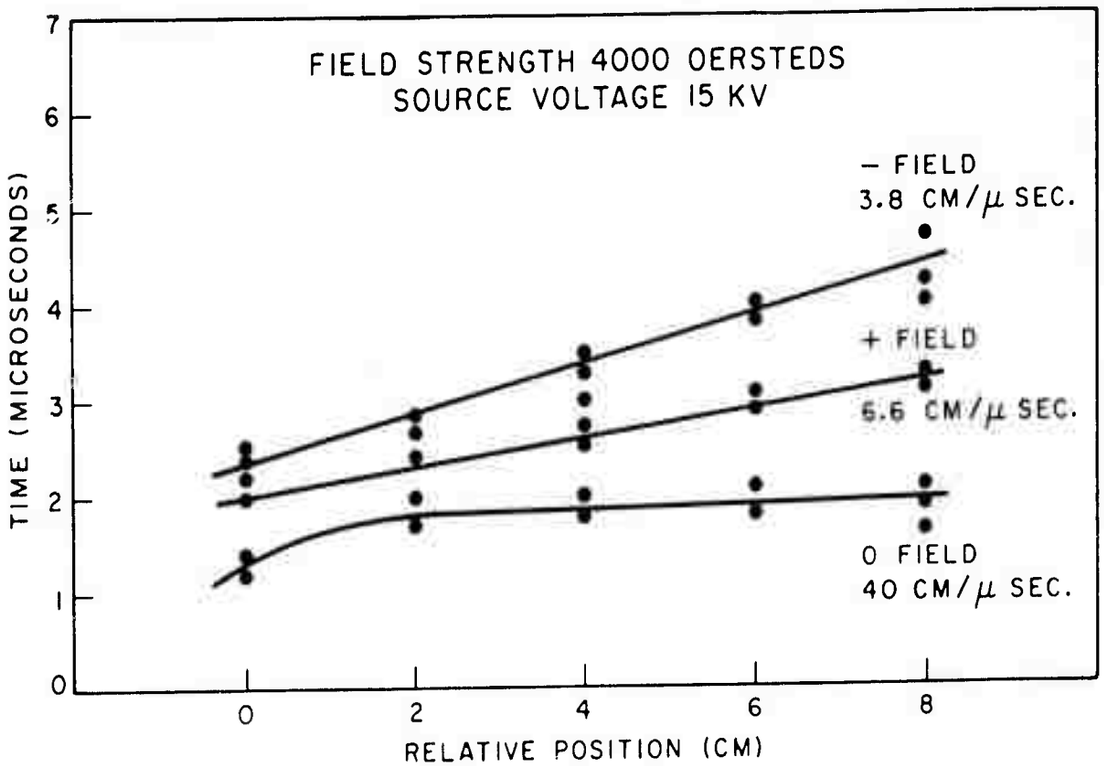

Figure 8. Arrival Time of Signal at Probe vs. Probe Position.

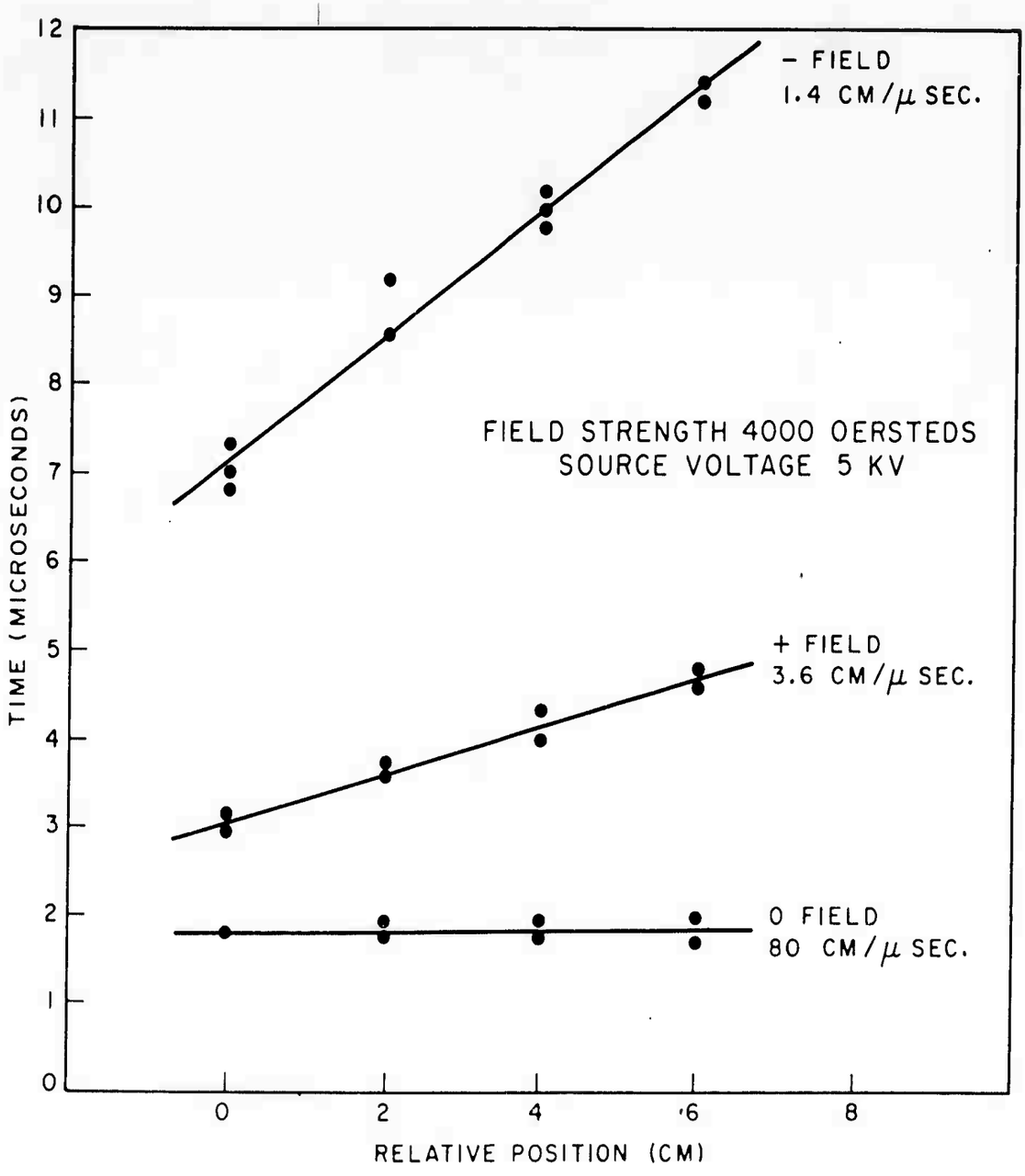

Figure 9. Arrival Time of Signal at Probe vs. Probe Position.

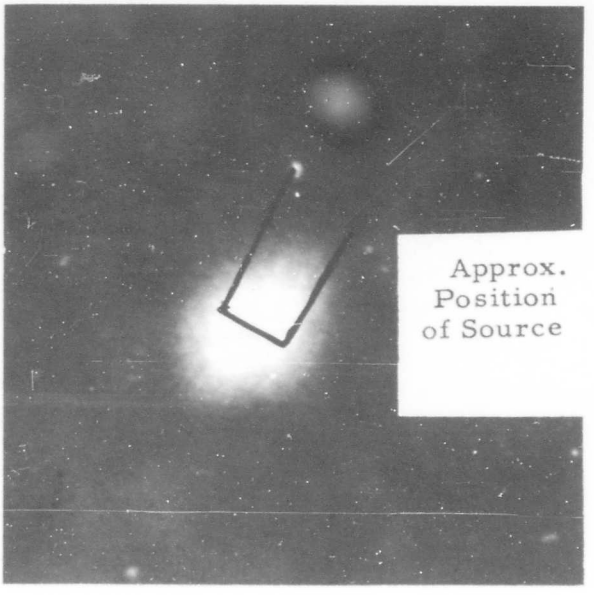

Figure 10. 0.2 μs Exposure 0.4 μs Delay

Figure 11. 0.2 μs Exposure 0.9 μs Delay

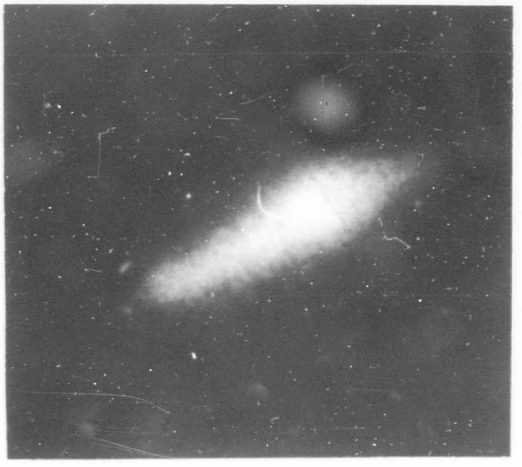

Figure 12. 0.2 μs Exposure 1.5 μs Delay

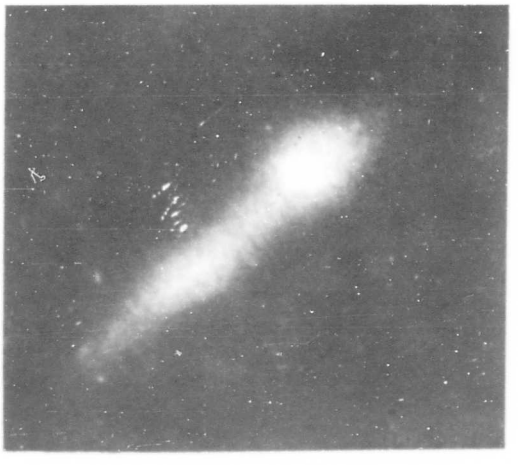

Figure 13. 0.2 μs Exposure 2.0 μs Delay

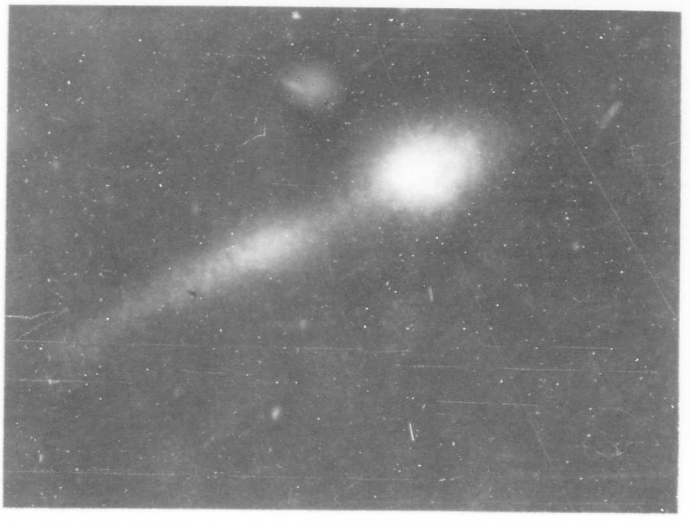

Figure 14. 0.2 μs Exposure 2.5 μs Delay

Figure 15. 0.2 μs Exposure 3.0 μs Delay

Figure 16. 0.5 μs Exposure 0.5 μs Delay

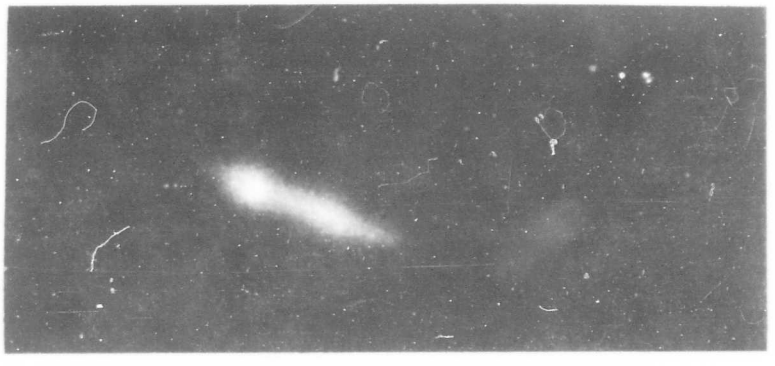

Figure 17. 0.5 μs Exposure 1.8 μs Delay

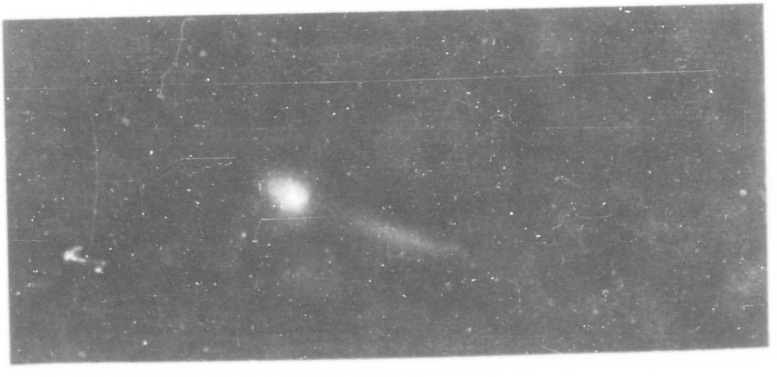

Figure 18. 0.5 μs Exposure 2.5 μs Delay

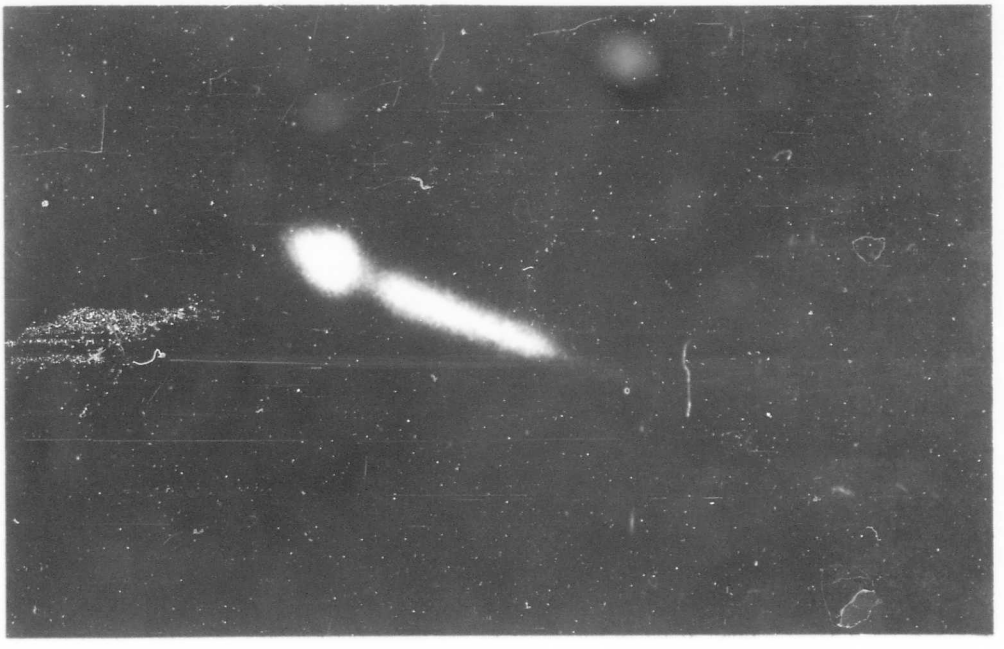

Figure 19. 2.0 μS Exposure 2.8 μS Delay

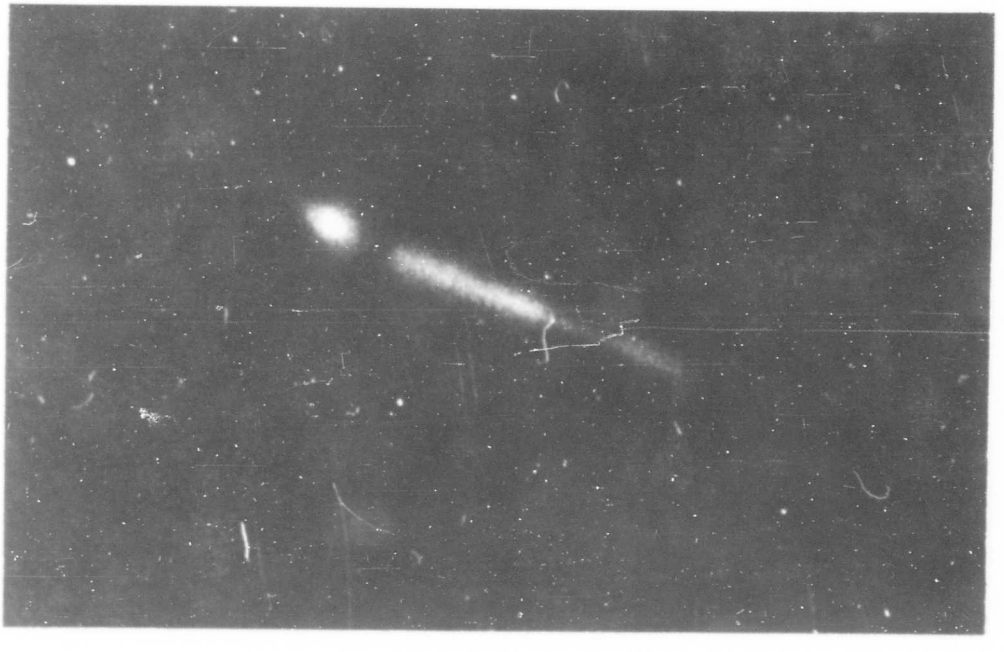

Figure 20. 2.0 μS Exposure 3.8 μS Delay

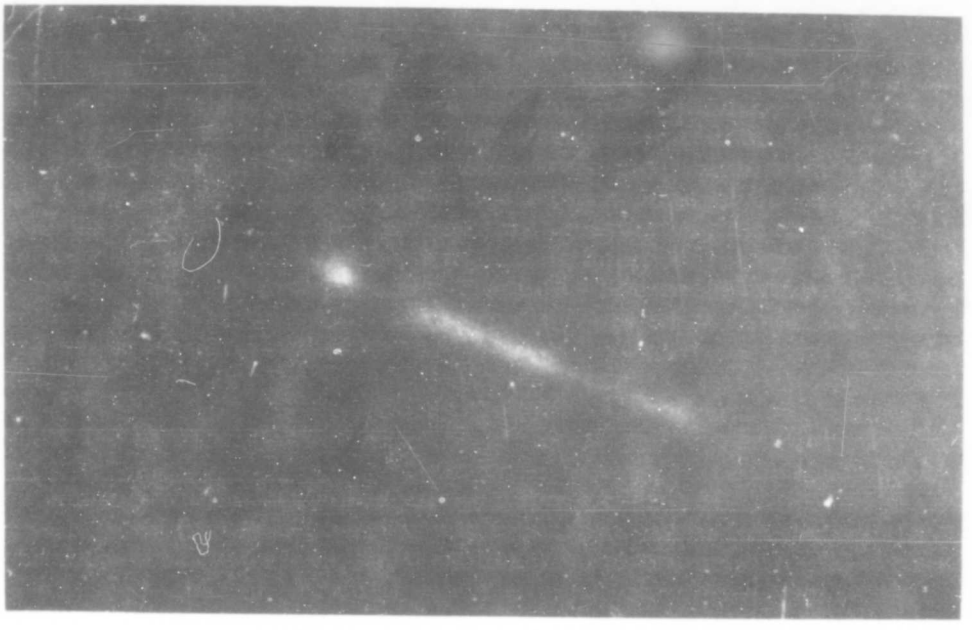

Figure 21. 2.0 μs Exposure 4.2 μs Delay

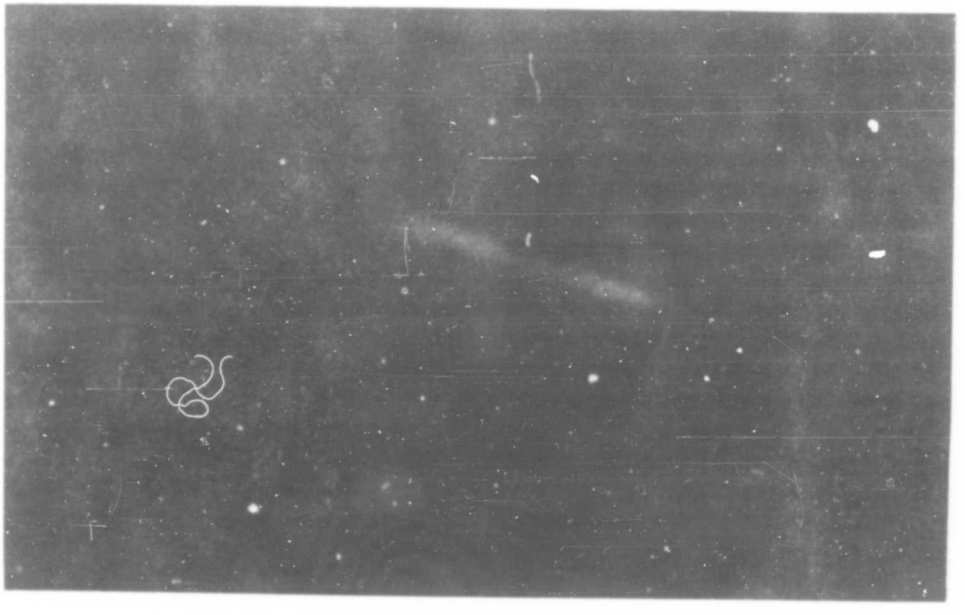

Figure 22. 2.0 μs Exposure 4.8 μs Delay

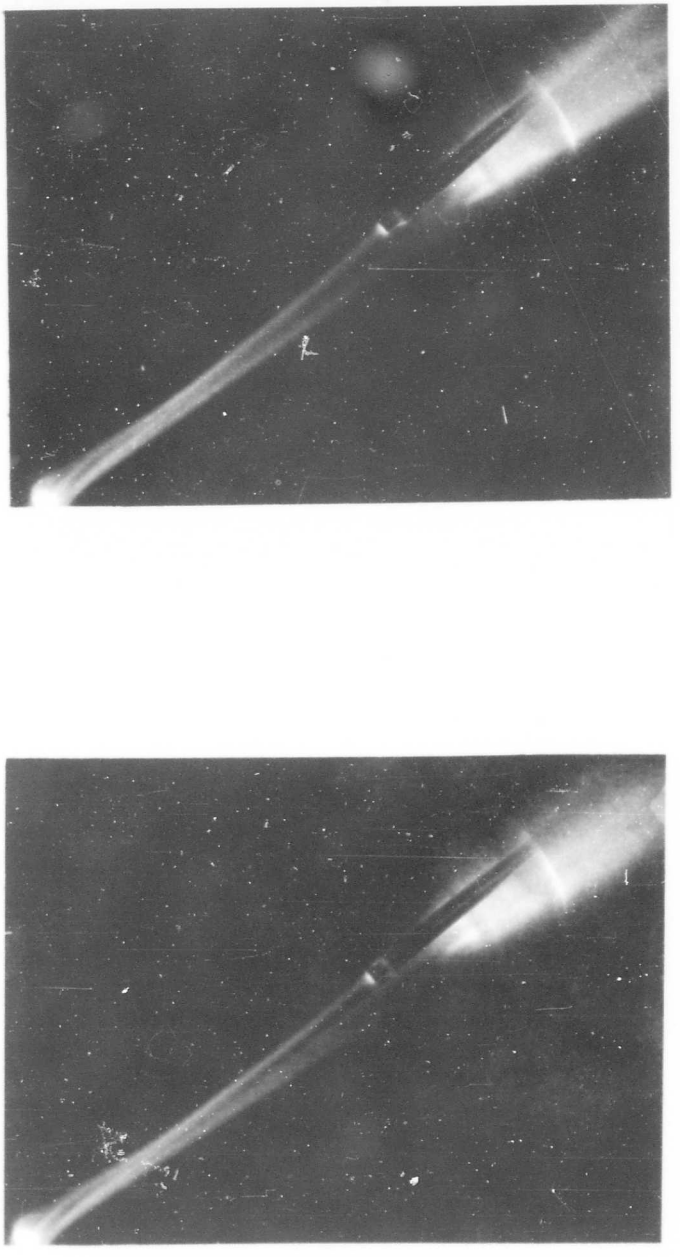

Figure 23. Plasma-Probe Interaction Field in the Positive Sense.

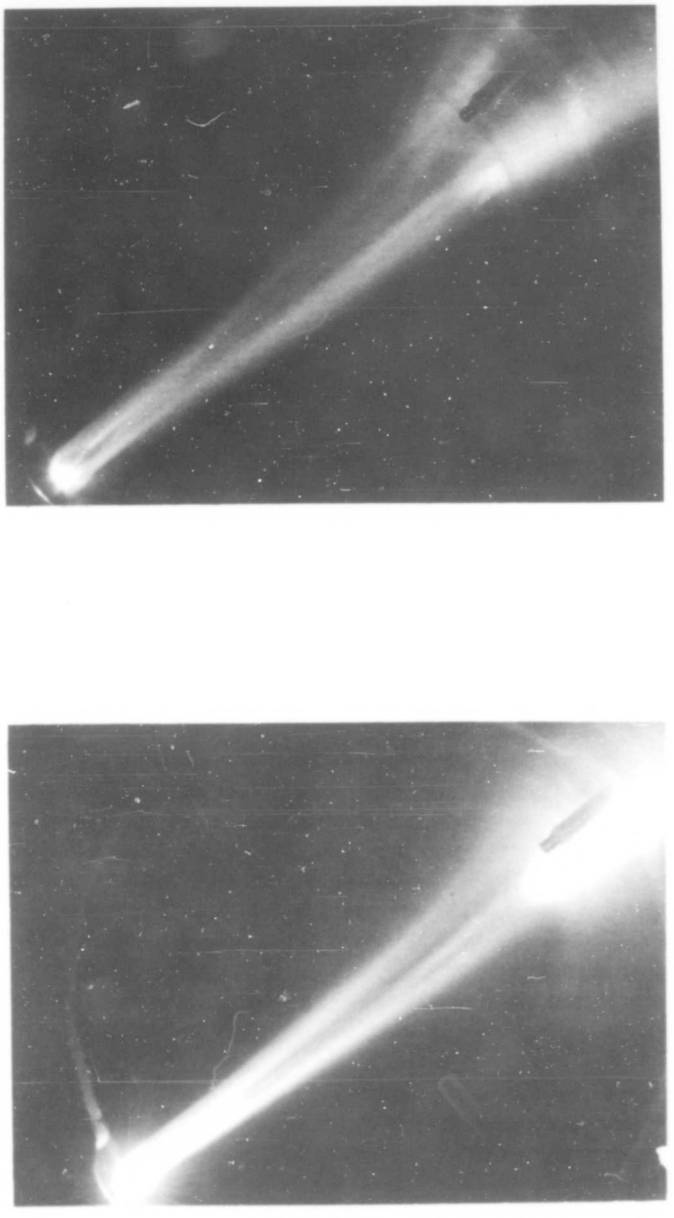

Figure 24. Plasma-Probe Interaction Field in the Positive Sense.

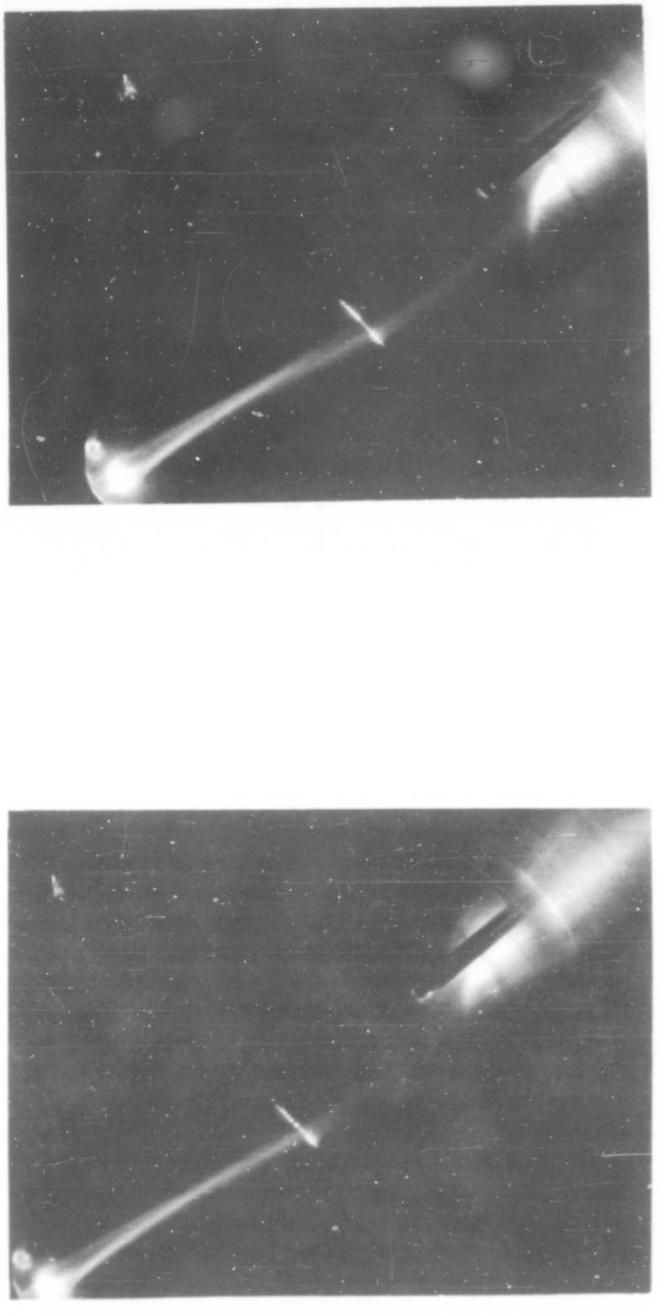

Figure 25. Interaction of Plasma with Wire Field in the Positive Sense.

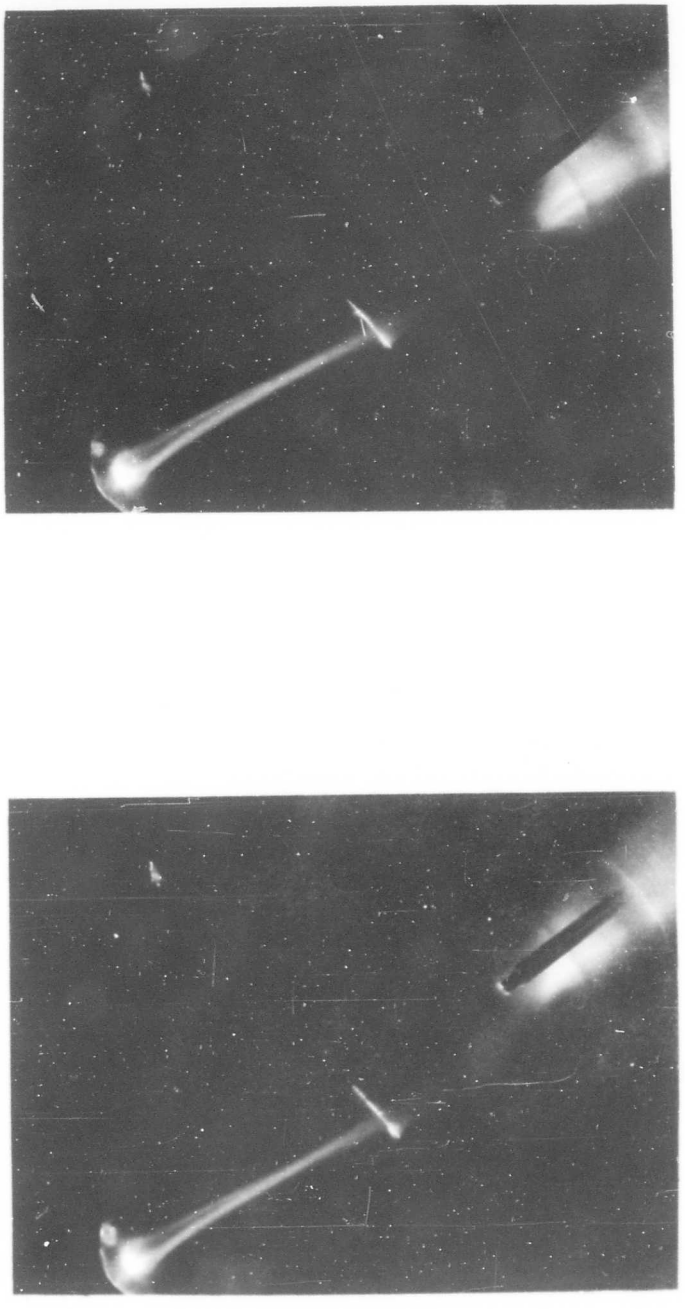

Figure 26. Interaction of Plasma with Wire Field in the Positive Sense

Figure 27. Interaction of Plasma with Probe Field in Negative Sense.

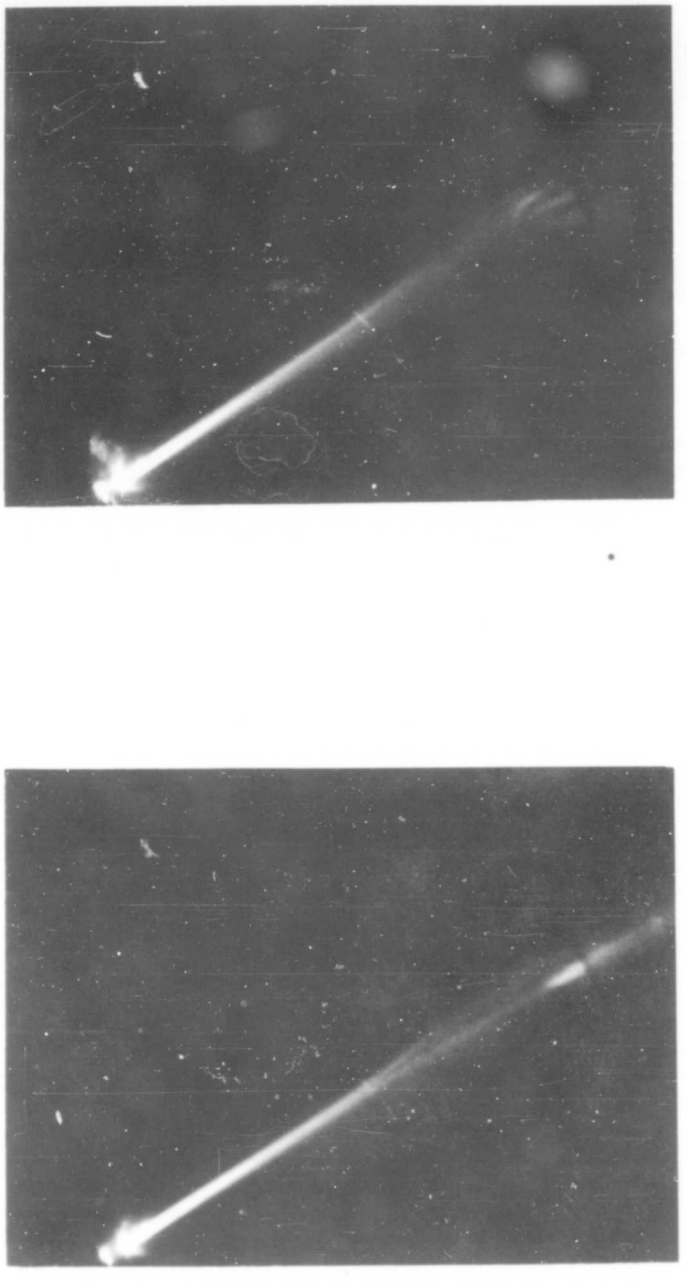

Figure 28. Interaction of Plasma with Wire Field in Negative Sense.

Back round field into paper
Self Field into paper

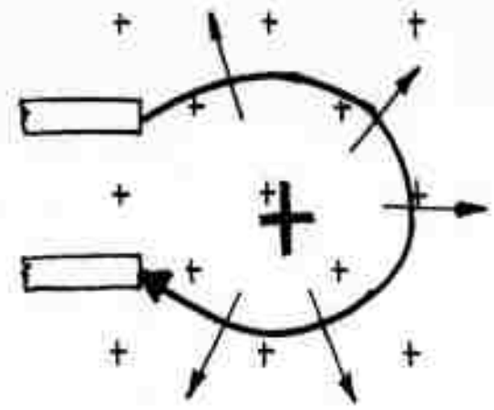

Plasmoid
Button
Electrodes

Net forces tend to expand the current loop.

a) Positive Field

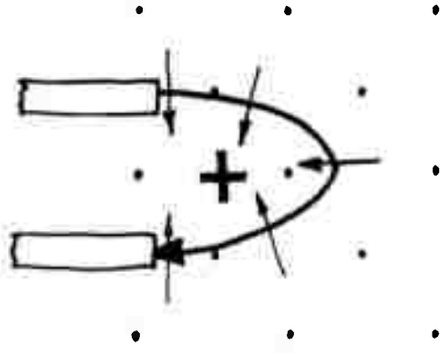

Back round field out of paper
Self field into paper

Net forces tend to compress loop

b) Negative Field

Figure 29 Forces on Arc Loops in Magnetic Fields

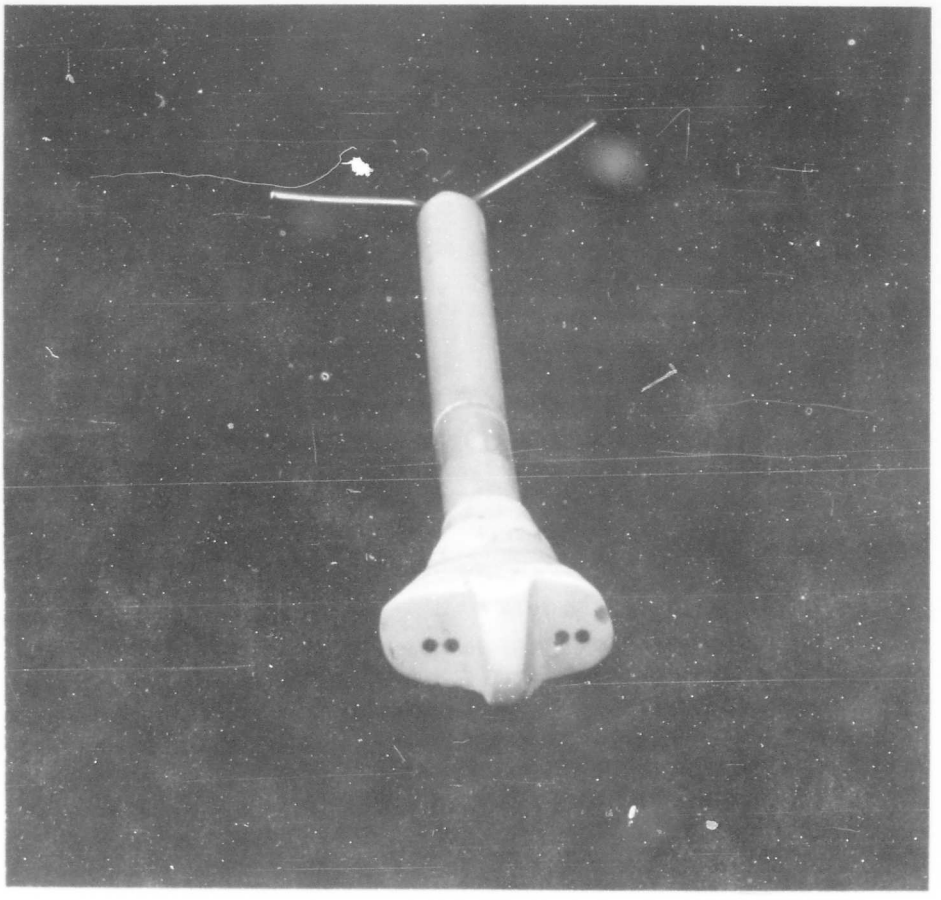

Figure 30. Dual Plasmoid Source

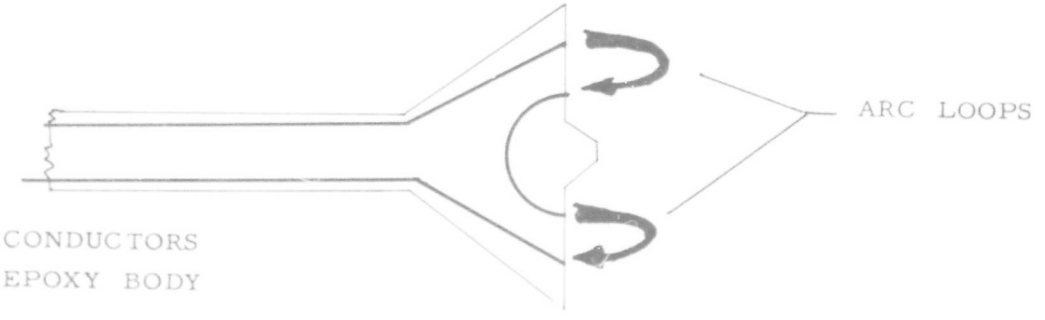

FIGURE 31. DUAL SOURCE (SCHEMATIC)

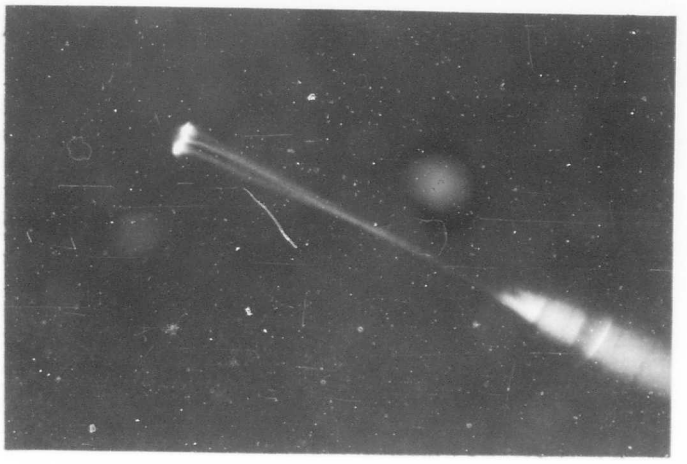

a) Maximum Positive Field - 15 Kv on Capacitor

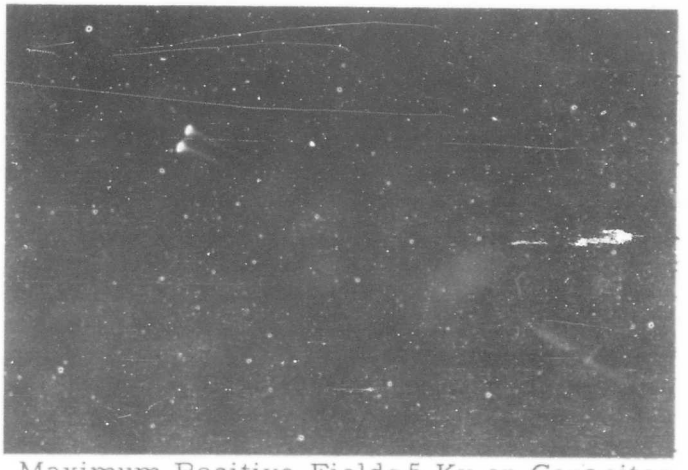

b) Maximum Positive Field - 5 Kv on Capacitor

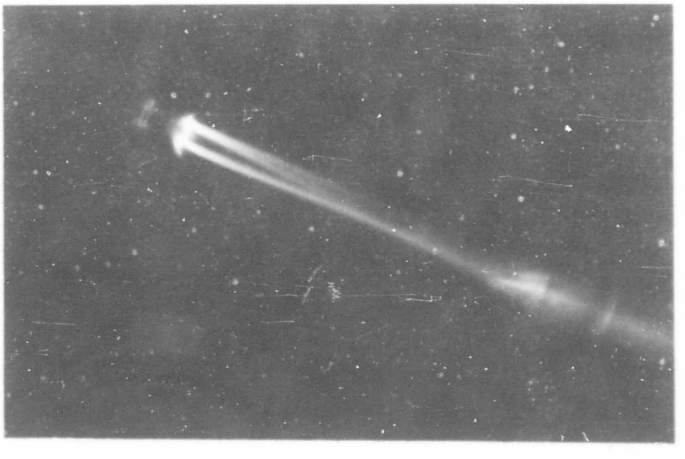

c) Maximum Negative Field - 15 Kv on Capacitor

Figure 32. Dual Plasmoid Trajectories

a) + $\frac{1}{2}$ increasing

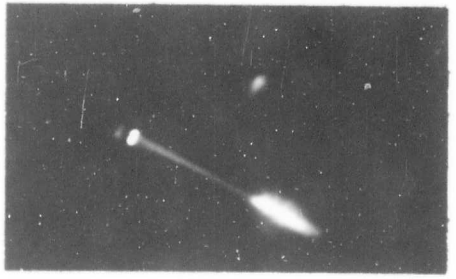

b) + 1 peak

c) + $\frac{1}{2}$ decreasing

d) O Field

e) - $\frac{1}{2}$ decreasing

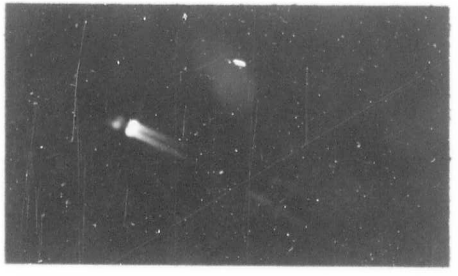

f) - 1 peak

g) - $\frac{1}{2}$ increasing

Figure 33. 2-Plasmoid Trajectories for Various Magnetic Fields.

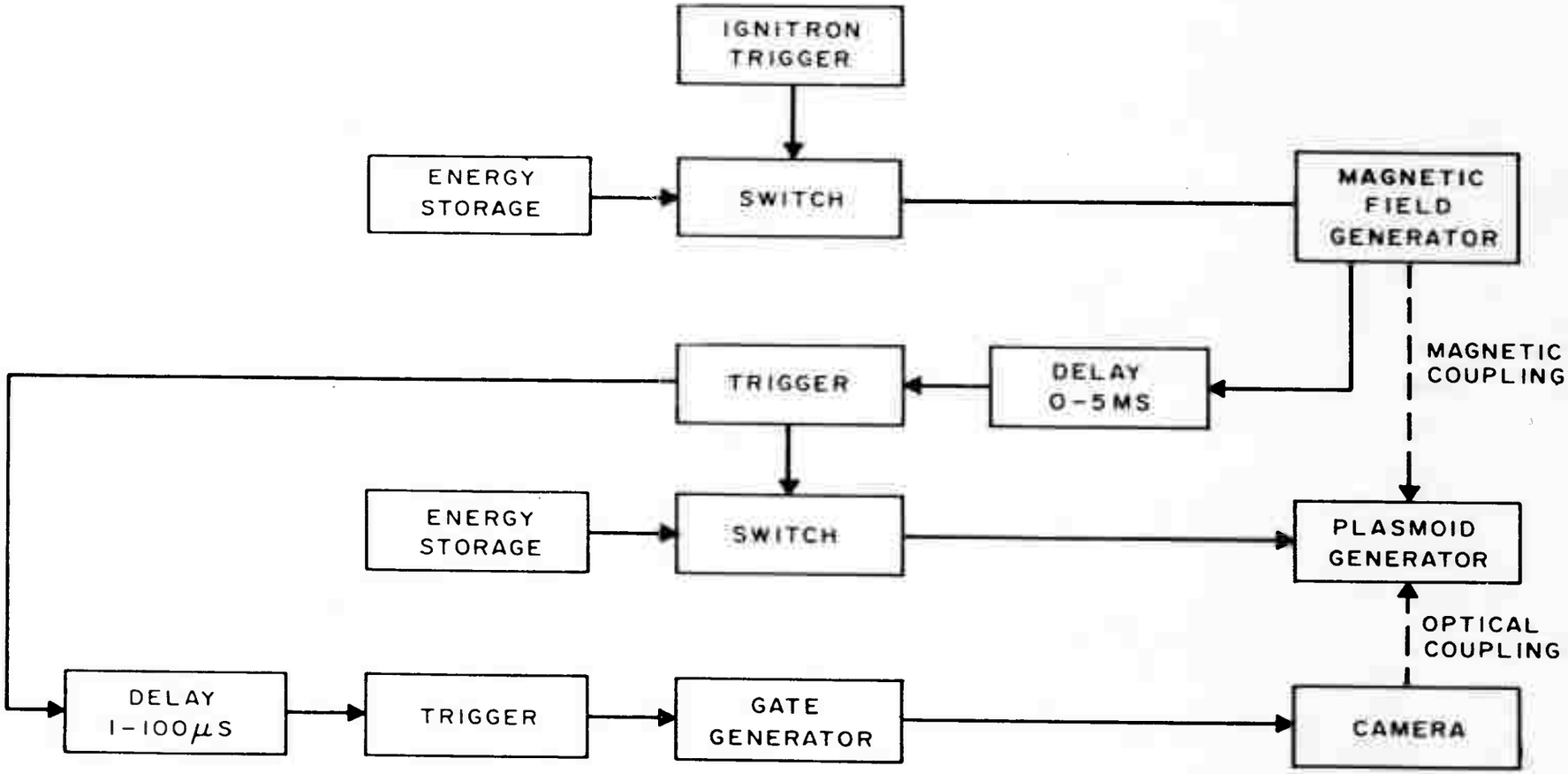

Figure 34. Block Diagram of System.

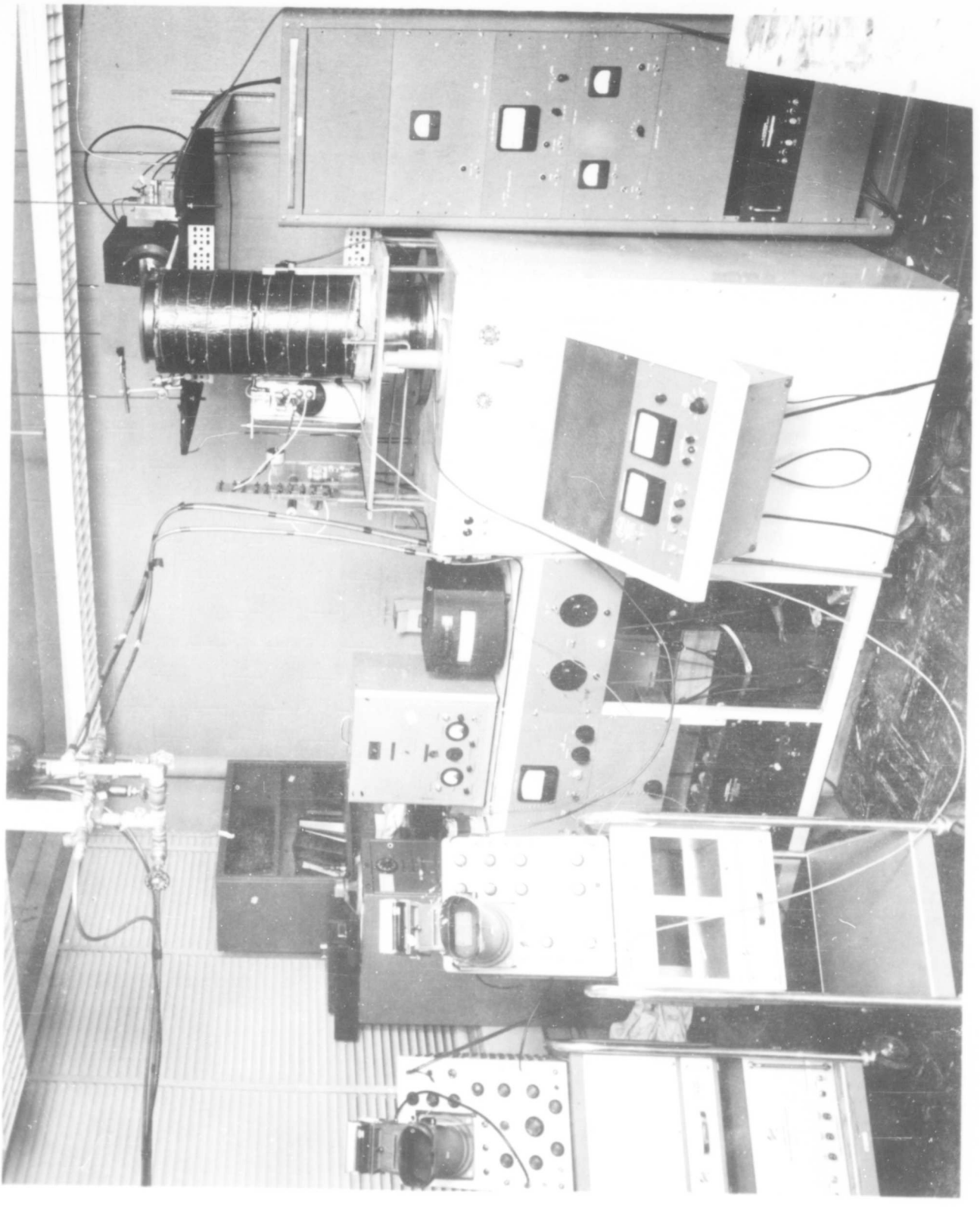

Figure 35. Experimental Apparatus

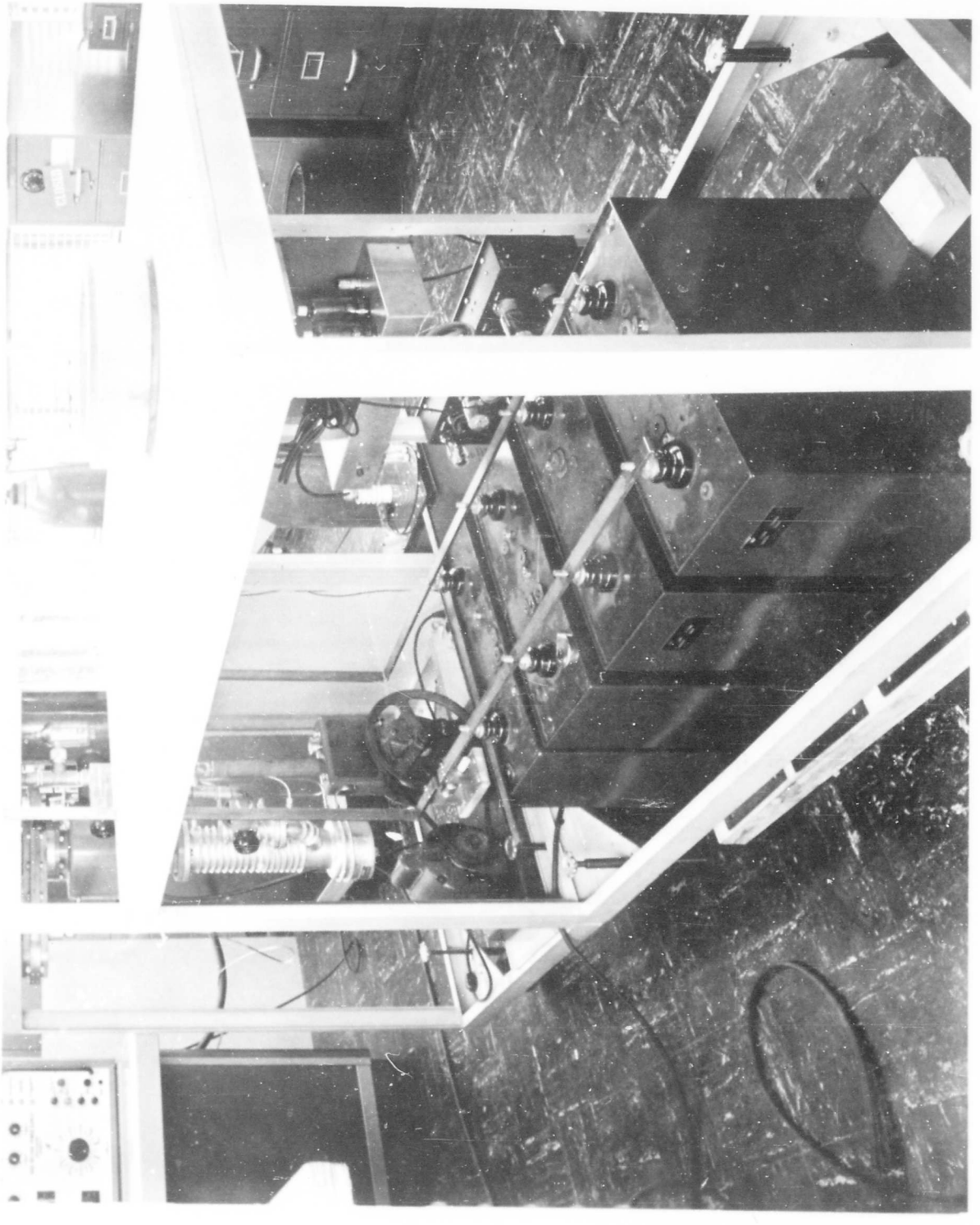

Figure 36. Capacitor Bank.

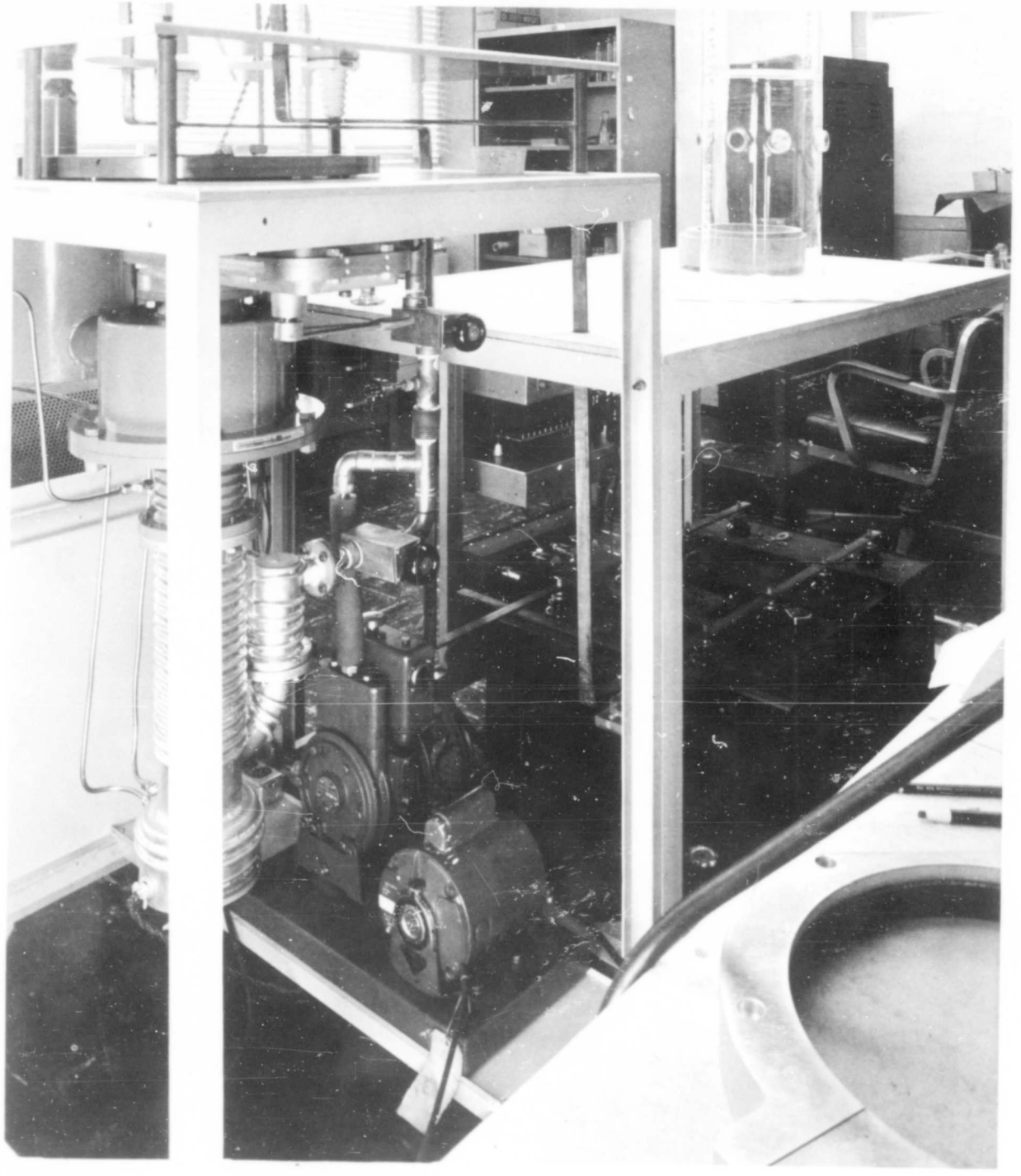

Figure 37. Vacuum System

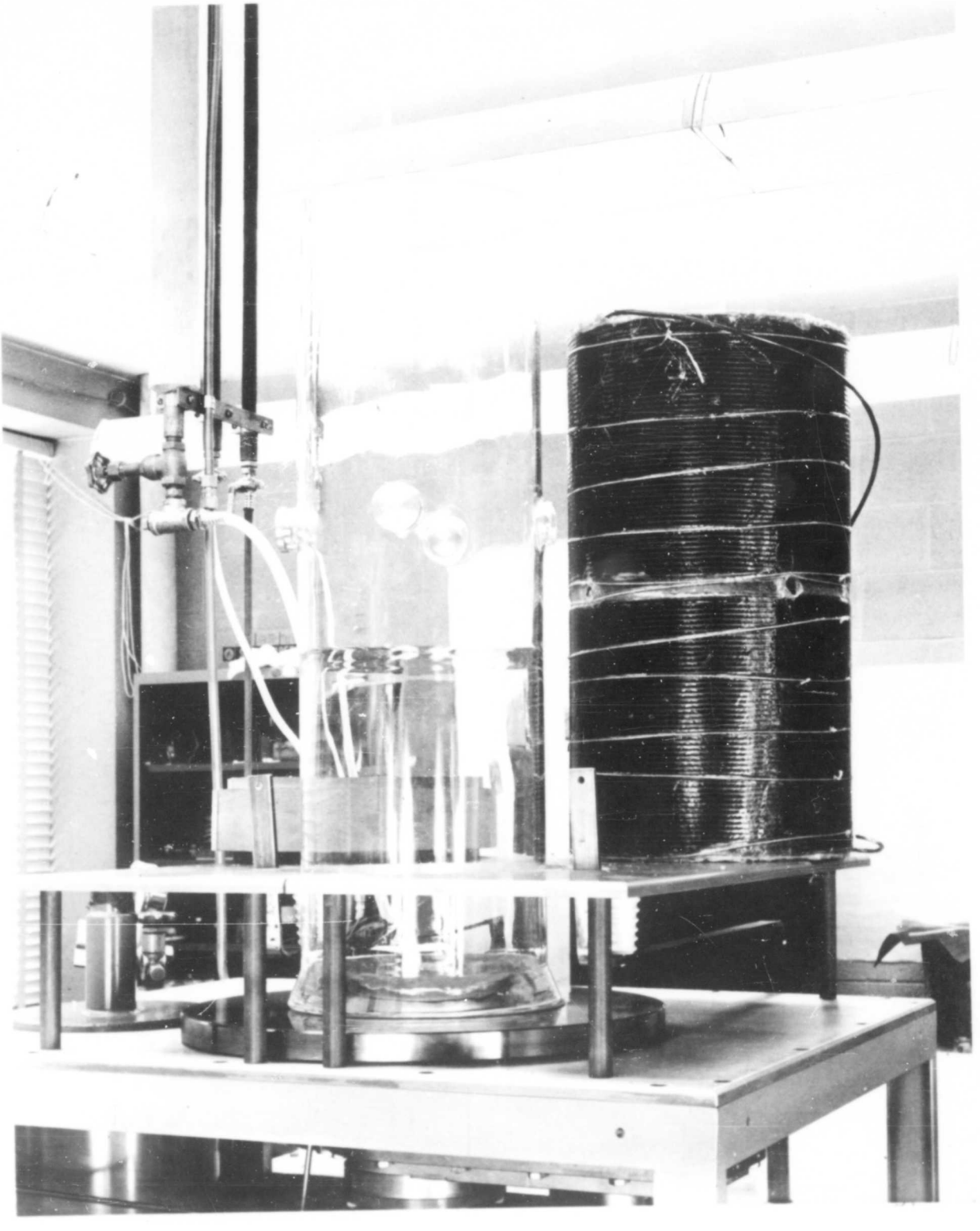

Figure 38. Vacuum Chamber.

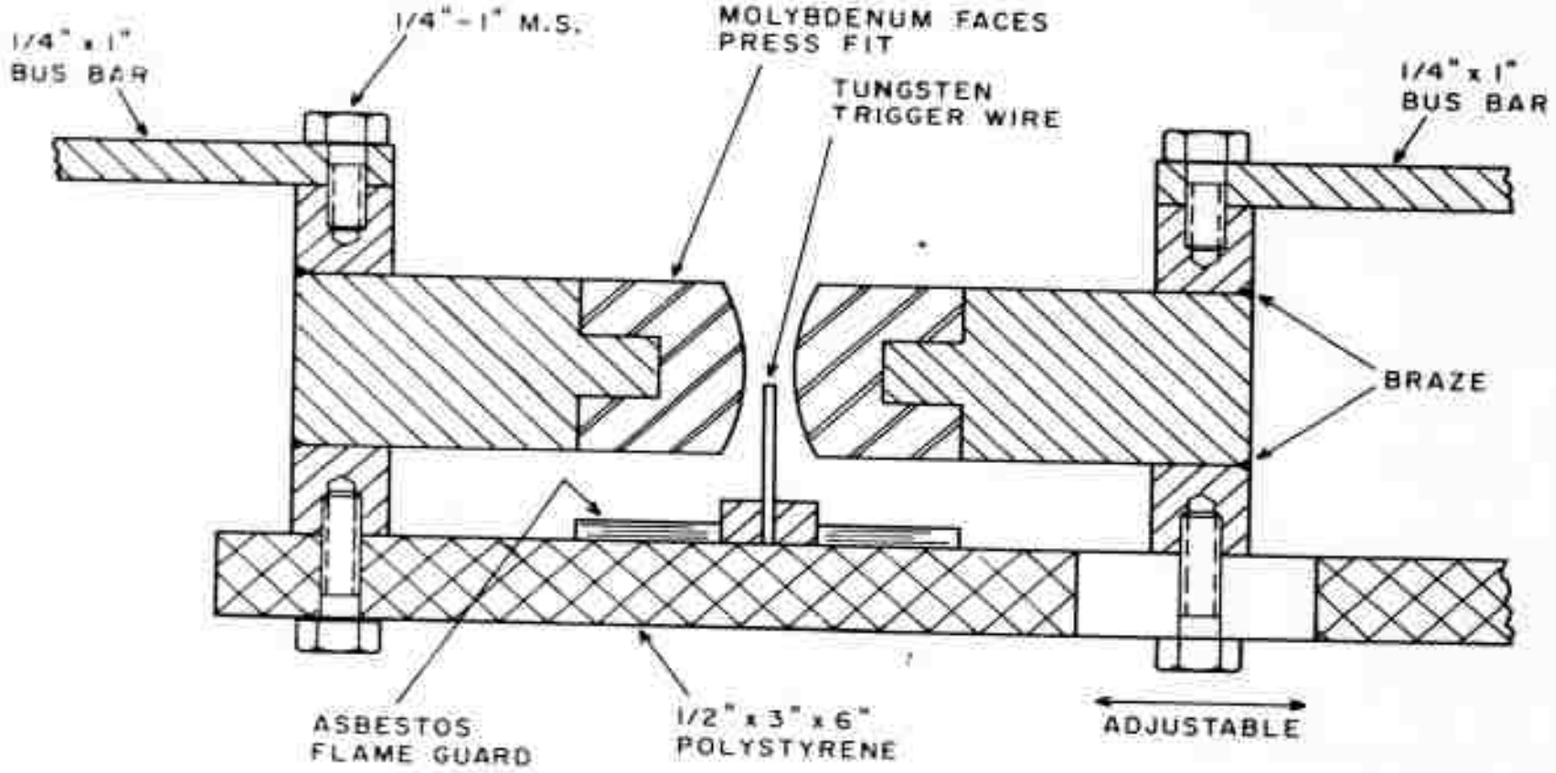

NOTE: ALL PARTS COPPER EXCEPT AS SHOWN. USE BRASS SCREWS.

Figure 39. Triggered Gap for Mayfield.

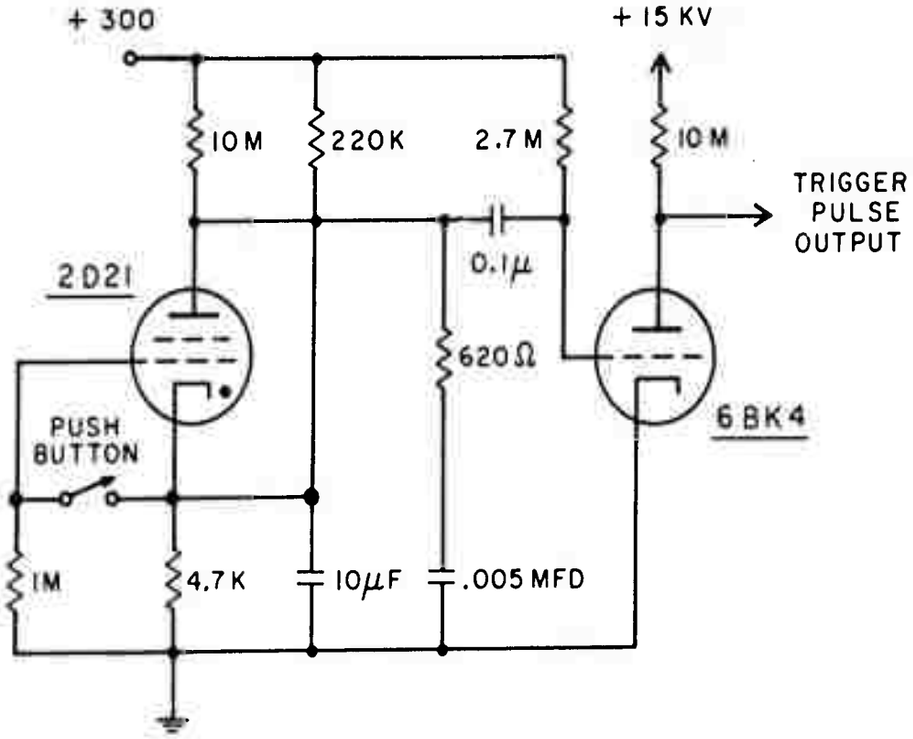

Figure 40. Trigger Circuit

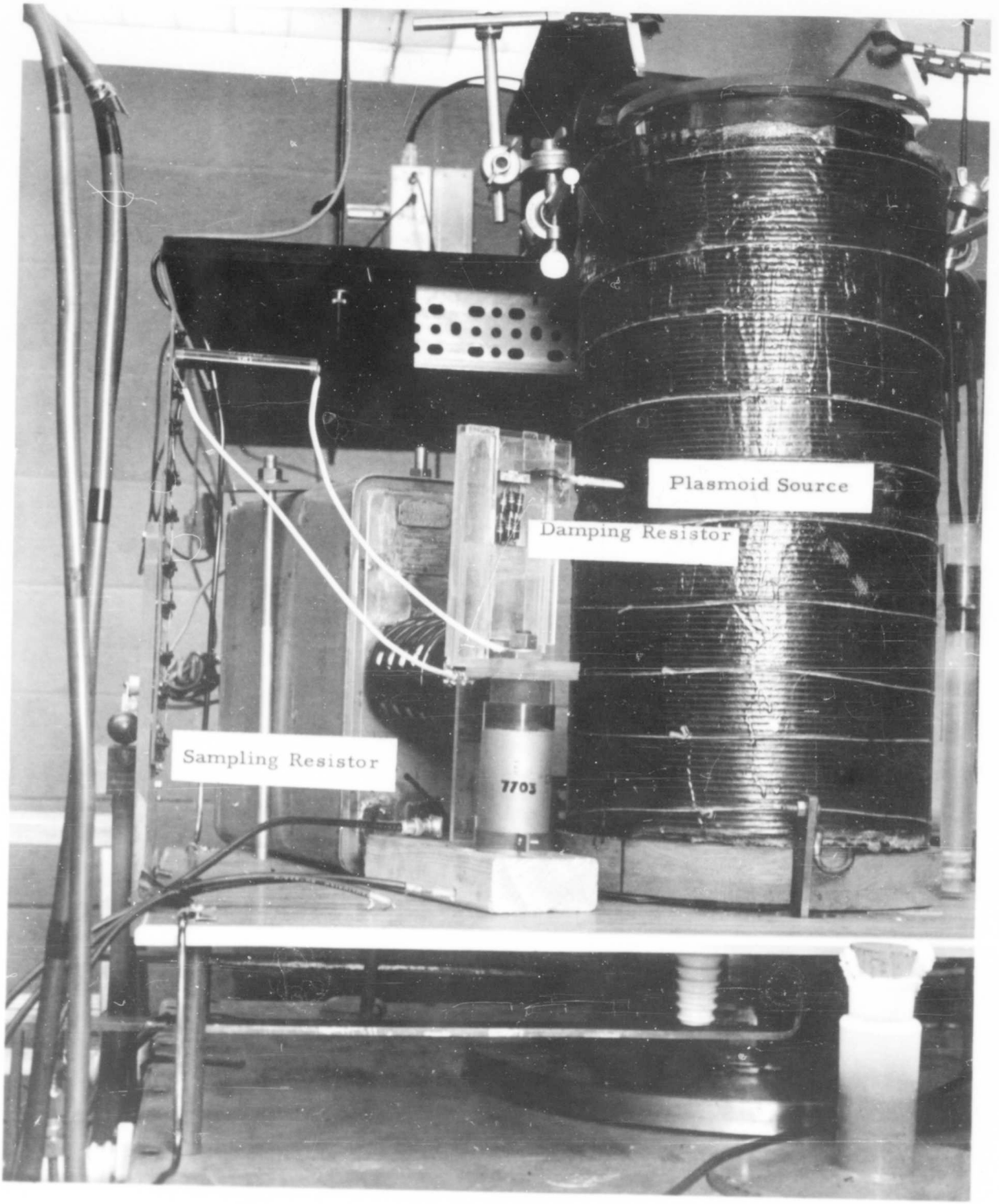

Figure 41. Ignitron Installation

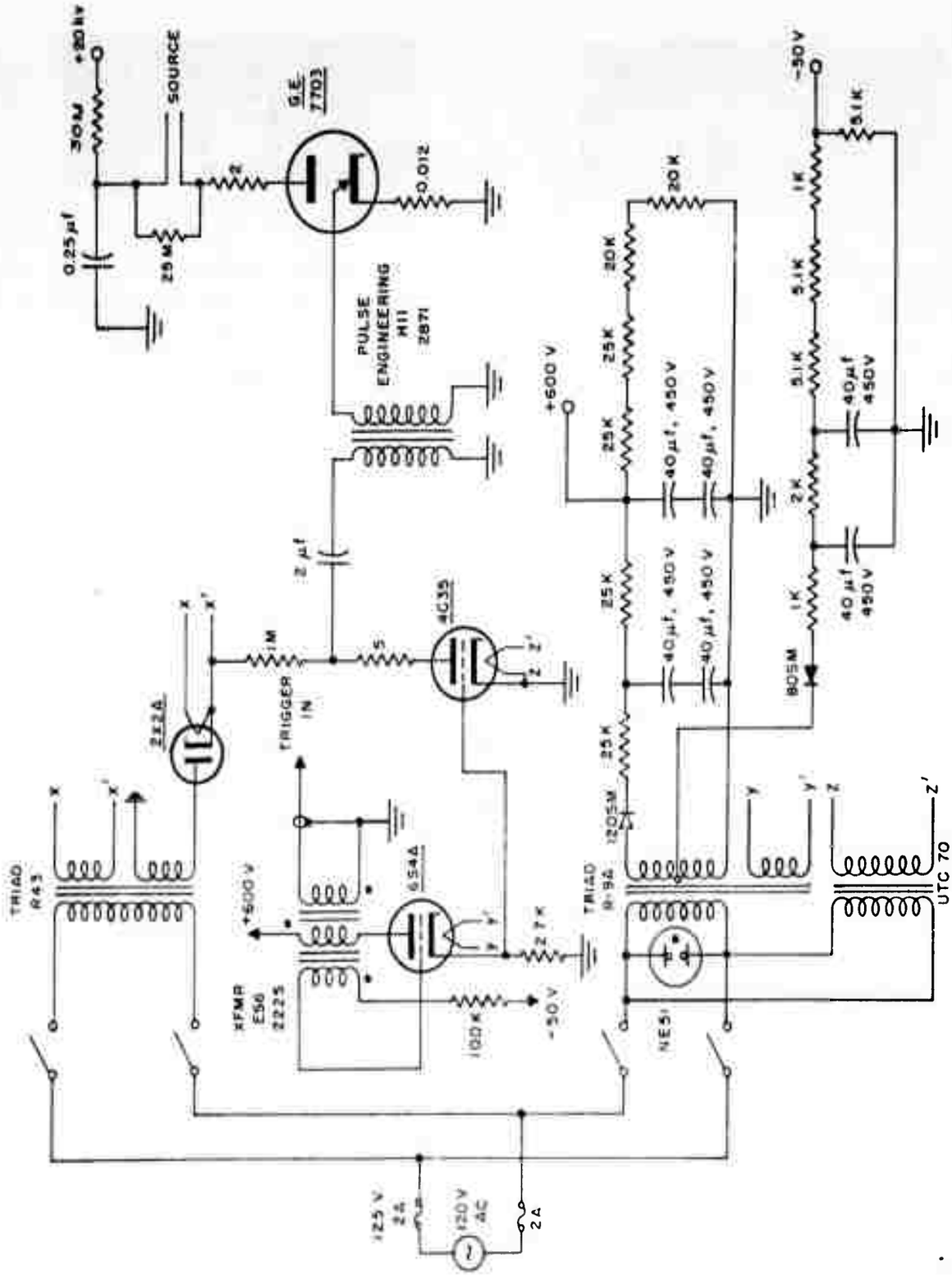

Figure 42. Ignitron Trigger Circuit

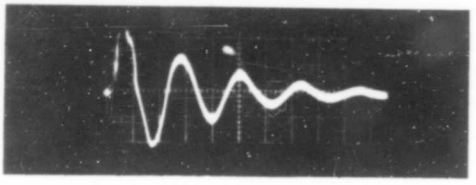

1. Free Current Waveform

Horz. Axis: 1 microsecond/division

Vert. Axis: ~ 5,000 amperes/division

13,000 A peak

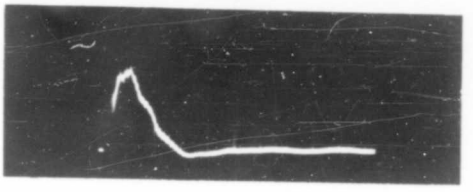

Damped Current Waveform

Horz. Axis: 1 microsecond/division

Vert. Axis: 2,170 amperes/division

6,500 A peak

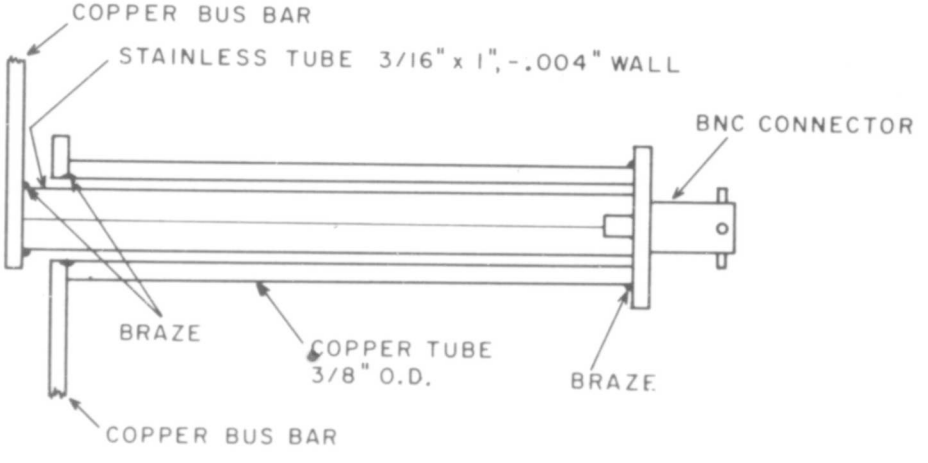

Figure 43. Current Sampling Shunt And Typical Waveform

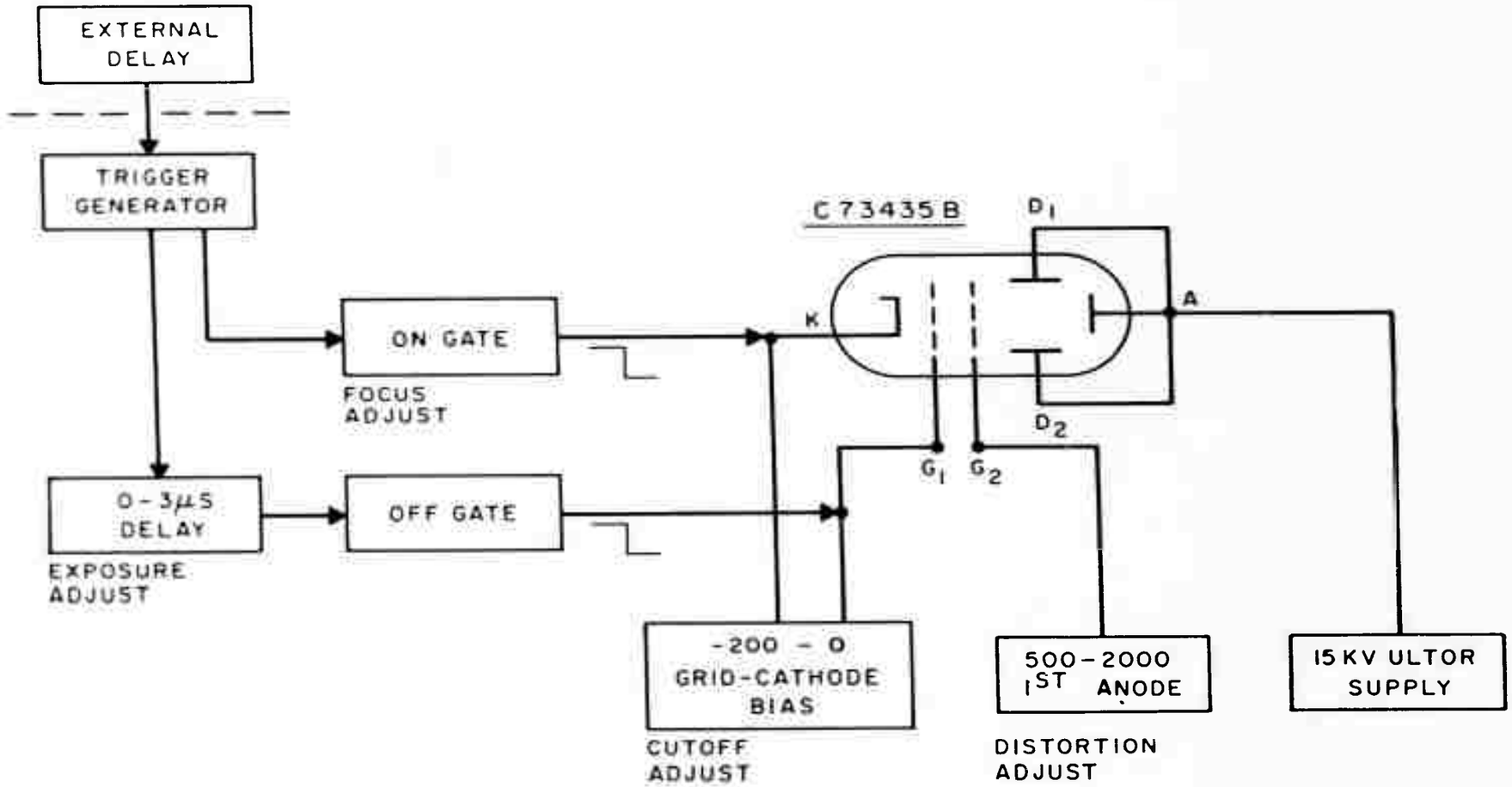

Figure 44. Camera Block Diagram.

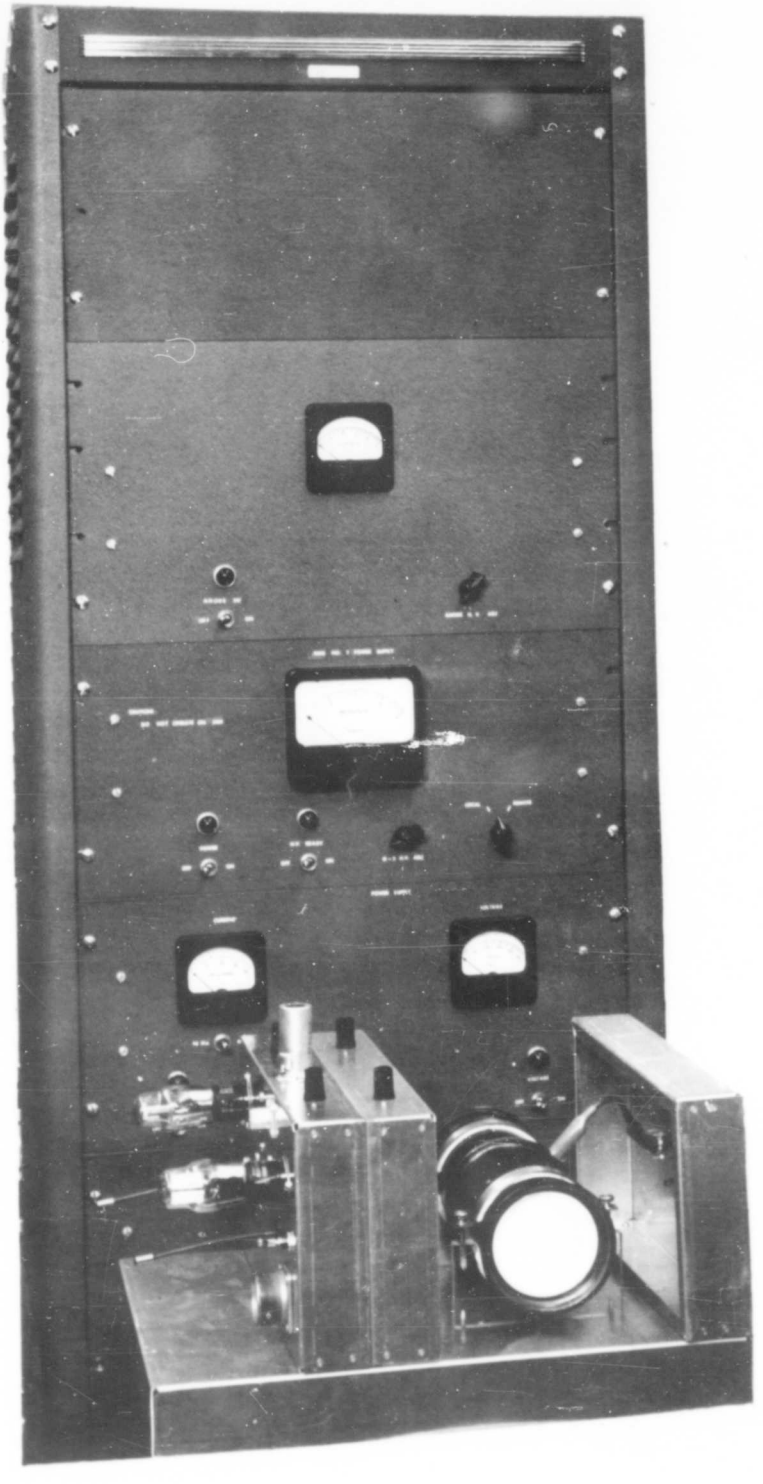

Figure 45. Overall View of Camera

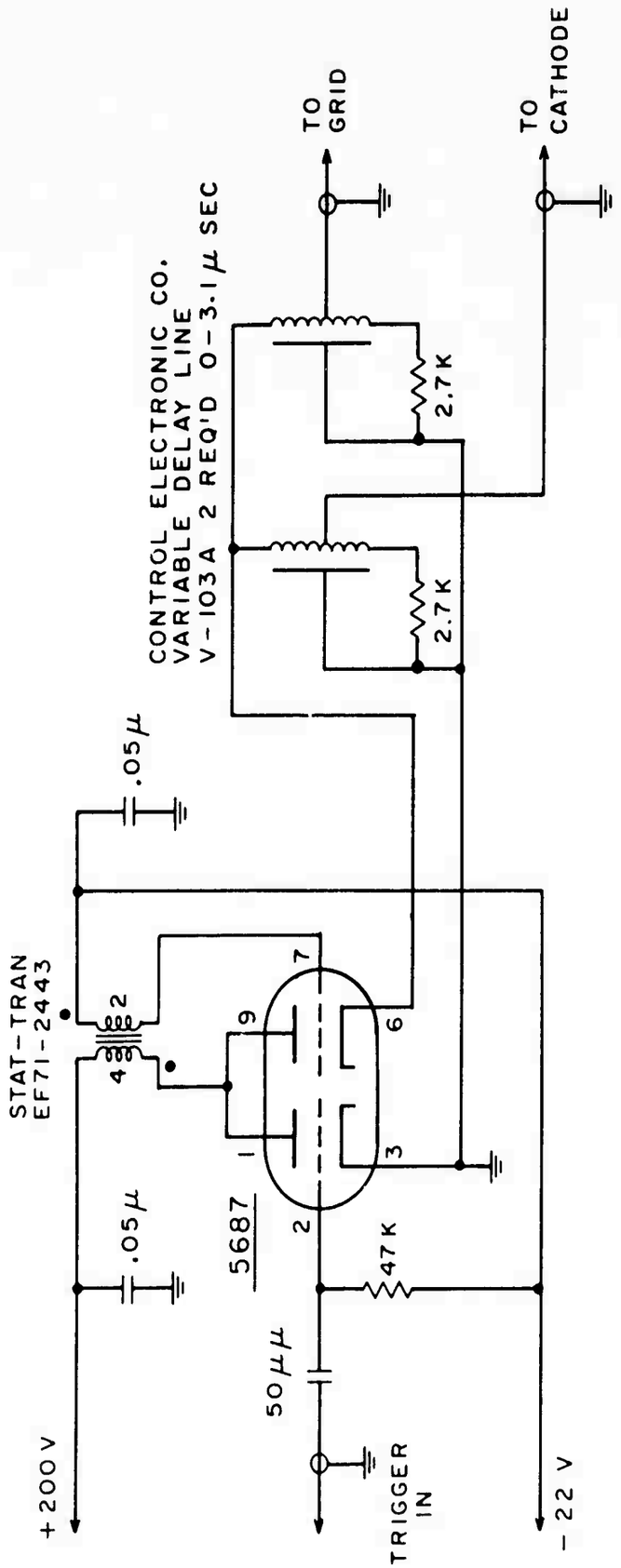

Figure 46. Blocking Oscillator and Delay Lines.

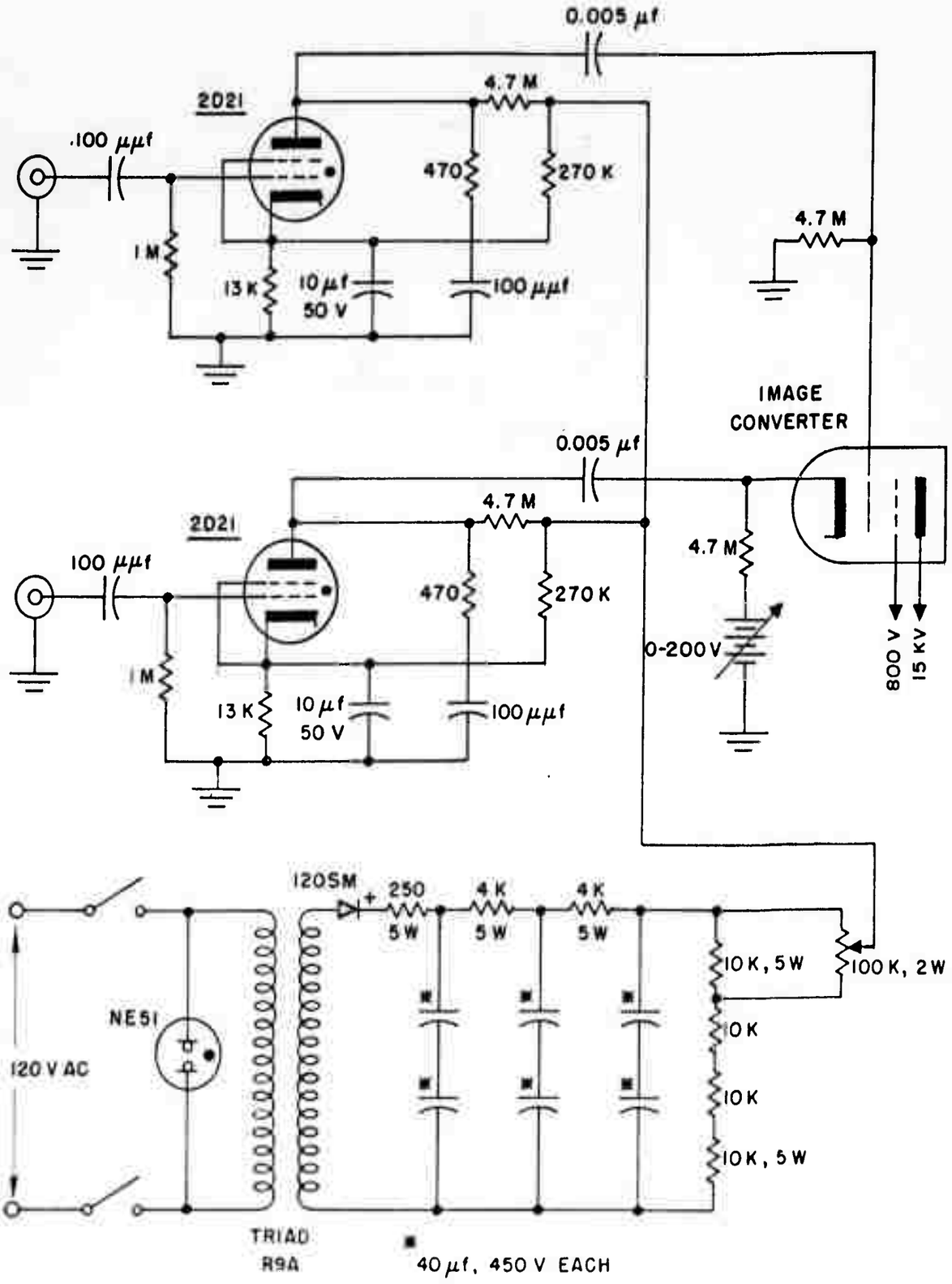

Figure 47. Thyratron Gate Circuits

UNCLASSIFIED